applied sciences

MDPI

Article

A Combined Forecasting System Based on Modified Multi-Objective Optimization for Short-Term Wind Speed and Wind Power Forecasting

Qingguo Zhou, Qingquan Lv * and Gaofeng Zhang

School of Information Science and Engineering, Lanzhou University, Lanzhou 730000, China; zhouqg@lzu.edu.cn (Q.Z.); gaofengzh@lzu.edu.cn (G.Z.)
* Correspondence: chwang2017@lzu.edu.cn

Abstract: Wind speed and wind power are two important indexes for wind farms. Accurate wind speed and power forecasting can help to improve wind farm management and increase the contribution of wind power to the grid. However, nonlinear and non-stationary wind speed and wind power can influence the forecasting performance of different models. To improve forecasting accuracy and overcome the influence of the original time series on the model, a forecasting system that can effectively forecast wind speed and wind power based on a data pre-processing strategy, a modified multi-objective optimization algorithm, a multiple single forecasting model, and a combined model is developed in this study. A data pre-processing strategy was implemented to determine the wind speed and wind power time series trends and to reduce interference from noise. Multiple artificial neural network forecasting models were used to forecast wind speed and wind power and construct a combined model. To obtain accurate and stable forecasting results, the multi-objective optimization algorithm was employed to optimize the weight of the combined model. As a case study, the developed forecasting system was used to forecast the wind speed and wind power over 10 min from four different sites. The point forecasting and interval forecasting results revealed that the developed forecasting system exceeds all other models with respect to forecasting precision and stability. Thus, the developed system is extremely useful for enhancing forecasting precision and is a reasonable and valid tool for use in intelligent grid programming.

Keywords: data pre-processing strategy; artificial neural network; multi-objective optimization algorithm; combined model

Citation: Zhou, Q.; Lv, Q.; Zhang, G. A Combined Forecasting System Based on Modified Multi-Objective Optimization for Short-Term Wind Speed and Wind Power Forecasting. *Appl. Sci.* **2021**, *11*, 9383. https://doi.org/10.3390/app11209383

Academic Editor: Amjad Anvari-Moghaddam

Received: 20 July 2021
Accepted: 23 September 2021
Published: 9 October 2021

1. Introduction

With the rise of globalization, renewable and alternative energy sources, which address security issues associated with conventional energy sources, are increasingly being favored to provide power for a wide range of social and economic activities. Wind energy, a promising technology utilized in many renewable energy systems, has attracted an increasing amount of attention in recent decades due to the drive to meet the rapidly growing electricity demand across the globe without emitting environmental pollutants, such as CO_2. According to the *GLOBAL WIND REPORT 2021* [1], China possesses 39% (278324MW) of the world's total onshore wind power capacity, and accounted for 56% of new onshore installations by the end of 2020, making it the world leader. As a result, the accurate forecasting of wind speed—the determining factor in wind energy electricity generation—has increasingly become a focus of public conversation, especially on the short-term horizon. Unfortunately, it is difficult to obtain excellent forecasting results because of the stochastic and nonlinear oscillations caused by uneven atmosphere stratification and complex topography [2].

In recent years, the capacity of onshore wind power sets has been rapidly increasing, which requires high reliability and maintainability in wind turbines with poor natural

conditions. Various methods have been developed to analyze wind turbine rotor blades. To identify the best-performing design for blade geometry, aerodynamic analyses are used to specify the desired radial distributions of the angle of attack, α (or sectional lift coefficient, cl) and axial induction factor along the blade and iterate the blade geometry (determined by the radial distributions of the blade chord, c, and twist, θ) until the required specifications are met. In aerodynamic evaluated processing, Selig and Tangler [3] use the blade element momentum (BEM) theory as for a method for aerodynamic analysis. Lee [4] used the vortex line method (VLM) and Moghadassian and Sharma [5] resolved Reynolds-averaged Navier–Stokes (RANS) equations using an actuator disk model (ADM) to emulate the rotor as a body force. These extensions permit analysis of unconventional rotor- and blade geometries, e.g., multi-rotor turbine configurations and rotor blades with dihedral and/or sweep. Meanwhile, the blade design of the wind turbine also affects the turbine output power coefficient (CP). For example, Tahani et al. [6] restricted the chord and twist distributions to linear profiles to increase the manufacturability of their design, and designed the rotor blade geometry (chord and twist) of a 1 MW wind turbine to maximize the CP. Liu et al. [7] investigated the blade design of a fixed-pitch, fixed-speed (FPFS) horizontal-axis wind turbine to maximize its annual energy production (AEP) for a prescribed wind speed Weibull distribution. They held the blade geometry fixed at the blade tip and assumed linear variations to reduce the design variables of the chord and twist values at the blade root.

Motivated by the need to urgently develop more precise measurement methods, a variety of studies have been conducted on wind speed forecasting over the past few decades. These studies can be broadly divided into two types: causal analyses and time series-based analyses [8]. Causal analyses use the established historical causality between explanatory and interpreted variables to forecast changes in future dependent variables [9]; however, such methods are prone to multiple collinear negative effects. Time series-based analyses can be subdivided into four approaches: physical [10], statistical [11], artificial intelligence [12], and hybrid [13] or combined models [14].

Advantages and shortcomings of those models include the following:

(1) For physical methods, to attain effective forecasting results, information on a range of physical factors is needed, rather than information on just a single factor such as the wind speed time series; thus, these meteorological models cannot generate forecasts simply [15]. In addition, physical models are not proficient in dealing with short-term series and involve a complex calculation process and high expansion costs, which all contribute to significant forecasting errors [16]. Physical models necessitate the gathering of numerical physical variables, such as the horizontal pressure gradient, geostrophic force, and fractionate to undergo wind speed forecasting [17]. However, the complex calculation and polytrophic processes involved are not only time consuming but create the risk of forecasting error [18].

(2) With sufficient accessible spatial and temporal information from multiple wind farms, a few spatio-temporal prediction methodologies have been able to be investigated in recent studies. The spatio-temporal characteristics of wind speed are extracted by an undirected graph of wind farms [19]. A hybrid support vector machine forecasting model is proposed, which is based on the spatio-temporal and grey wolf optimization, to forecast wind power for multiple wind farms [20]. Ref. [21] uses copula theory and Bayesian theory to simulate spatio-temporal correlations between wind farms and deduce a conditional distribution of aggregated wind power. A probabilistic wind speed prediction approach was presented in Ref. [22] based on a spatio-temporal neural network (STNN) and variational Bayesian inference. With feeding of both the spatial and temporal information into the forecasting model, these methods have achieved a better forecasting performance. Nevertheless, most of these forecasting models often collected the wind speed information from different wind farms indiscriminately, and to some extent, the implicit spatial correlations cannot be fully exploited in the original wind speed data. Also, the thorny multi-dimensional computing problem

caused by the large amount of wind speed data from multiple wind farms needs to be solved in an effective way.

(3) Typical statistical methods can yield excellent forecasting results under the assumption that the input series was recorded under normal conditions [23]; however, nonlinearity, noise, instability, fluctuations, and other features within the raw time series are always difficult to control, resulting in a lack of modeling information. Therefore, such methods often result in bad short-term wind speed forecasting performance, especially in multistep-ahead forecasting [24]. In addition, historical data are utilized for statistical modeling methods, and only potential linear correlations between the variables and future forecasts are revealed; such models are unable to obtain a good forecasting performance within the required limits [25]. Statistical models, including typical autoregressive moving average family models (e.g., AR [26], MA, ARMA [27], autoregressive integrated moving average models (ARIMA) [28], SARIMA, etc.), exponential smoothing [29], Kalman filtering [30], vector autoregression structures for very short-term wind power forecasting [31], and autoregressive conditional heteroskedastic family models (e.g., ARCH, GARCH, and EARCH) [32] utilize significant amounts of historical data for wind speed forecasting with no consideration of other potential influencing factors to support the stochastic process. Meanwhile, a spatial-temporal forecasting method based on the vector autoregression framework has been proposed for renewable forecasting [33]. Generally, statistical methods work well for approaching linear features; however, they tend to fail when it comes to nonlinear problems due to the linear assumptions of the models [34].

(4) Fortunately, the timely emergence of artificial intelligence (AI) arithmetic, subsuming artificial neural networks (ANNs) [35], support vector machines (SVMs) [36], deep neural networks [37], and fuzzy logical methods (FLMs) [38] have efficiently remedied the flaws in the wind speed forecasting territory in recent years [39]. However, because of the inherent disadvantages of each model and the boom in the integration of wind power into the grid system, a variety of hybrid and combined models with promising forecasting potentials have been created [40]. Generally, artificial intelligence methods can achieve greater forecasting accuracy than physical or statistical models [41]; however, they also possess insurmountable drawbacks. ANNs have been extensively studied and applied to explore the complexity of wind speed forecasting; however, their performance mostly relies on training sets, which can result in a focus on local optima, over-fitting, and a reduction in the convergence rate [42].

(5) Differently to conventional or single models, hybrid models can reduce the current shortcomings associated with the forecasting of irregular, fluctuant, and nonstationary time series with noise or unpredictable components. In this regard, significant hybrid models have recently been launched [43]. Hybrid methods integrate different single algorithms to achieve a superior forecasting performance, and can overcome defects in AI models (e.g., falling into local minima, over-fitting, etc.)—greatly improving the accuracy of continuous fluctuant wind speed forecasting and providing better validity and stability than a single model [44]. Recently, the use of hybrid methods in the wind speed forecasting field has been widespread. Jiang et al. [45] proposed a hybrid model consisting of a grey correlation analysis, cuckoo search algorithm, and v-SVM (v-support vector machine). Dong et al. [46] proposed a hybrid preprocessing strategy coupled with an optimized local linear fuzzy neural network for wind power forecasting. It has been proven that this is a effective approach for predicting wind power. In 2017, Hu et al. [47] proposed a novel approach based on the Gaussian process with a t-observation model for short-term wind speed forecasting. Based on a spatio-temporal method, in [48], the performance of predictive clustering trees with a new feature space for wind power forecasting was investigated. The results showed that the proposed model achieved a satisfactory level of point forecasting accuracy and interval forecasting performance. A forecasting framework has been proposed in 2021 [49], that is multi-layer stacked bidirectional long/short-term memory (LSTM)-

based for short-term time series forecasting. After being studied extensively, it is clear that no arithmetic method is omnipotent across all data cases. In future research, individual statistical models and artificial intelligence algorithms will be integrated to improve the precision of wind speed forecasting—these are referred to as hybrid models [50].

As mentioned previously, conventional or individual methods always show inherent weaknesses when approaching complex and actual wind time series with noise, which results in poor forecasting performances.

In accordance with previous studies, we designed three procedures for wind speed and wind power forecasting. First, data preprocessing was employed to identify features and eliminate useless information from the original time series. Then, the preprocessed time series was used to train and test the multi-artificial neural network. The models were ranked based on the test set accuracy for each model. Finally, the top five models were used as sub-models of the combined model. To obtain stabilized and accurate forecasting results, the weight of the combined model was optimized by the multi-objective optimization algorithm, which improved the stabilization and accuracy of the combined model.

The key findings of this study and comparisons with relative research in the field of wind speed forecasting are as follows:

(1) To achieve accurate and stable forecasting of short-term wind speed and wind power, a robust, novel, combined system based on three modules was developed in this study. This novel hybrid system for forecasting short-term wind speed and wind power includes a data preprocessing module, a forecast optimization module, and an evaluation module. The excellent performances of these algorithms are combined to provide accurate and stable results for multi-step wind speed forecasting.

(2) To effectively eliminate fluctuations in the original time series and avoid the limitations of a single algorithm, a new data preprocessing step was proposed. This was shown to decrease uncertainty and irregularity in the wind speed times series. SSA-EEMD, a powerful secondary denoising algorithm, was used to decompose and further denoise the actual wind speed time series. These steps were found to successfully overcome the limitations of single SSA algorithms.

(3) To overcome the disadvantages of individual models, multi models were used to forecast the wind speed and wind power. To consider the nonlinear characteristics of wind speed and wind power time series, seven artificial neural networks (ANNs) were employed to forecast two types of time series, and five optimal hybrid models were selected based on the accuracy of data testing by hybrid models to form a combined model and act as sub-models.

(4) To further improve forecasting accuracy and stability, the multi-objective dragonfly algorithm was used to determine the optimal weight of the combined model. In the optimization process, the optimized parameters were found to not only have good accuracy, but they also ensured that the output results had a high level of stability. Therefore, this paper used the multi-objective optimization algorithm to optimize the weight of the combined model.

(5) A more scientific and comprehensive forecasting evaluation method was conducted to estimate the forecasting performance of the developed forecasting system in the model evolution module. Interval forecasting was used to assess the uncertainty of the combined model, and this indicated that the forecasting results of the proposed combined model were accurate and stabilized in an all-around manner. Additionally, the Diebold–Mariano test and Wilcoxon rank-sum test were implemented to further analyze the forecasting accuracy of each model.

The remaining sections of this paper are as follows: The methods involved in the proposed model are introduced in Section 2. Section 3 demonstrates the experiment preparations and the four numerical experiments used, as well as presenting the forecast results. Deeper discussion about the forecasting performance of our developed model is presented in Section 4. Section 5 provides the conclusions.

2. Flow of the Proposed Combined Model

In the 1960s, J.M. Bates et.al. discovered combined forecasting methods, which use more than two different forecasting models to address the same problem. Multiple models can be combined by the combination of quantitative methods. The main purpose of this combination is to make full use of the information provided by various models to improve forecasting accuracy [51]. In our study, a combined forecasting model was developed to forecast the nonlinear characteristics of wind speed and wind power. The forecasting processes used are shown in Figure 1, and the details of the forecasting procedure are described below.

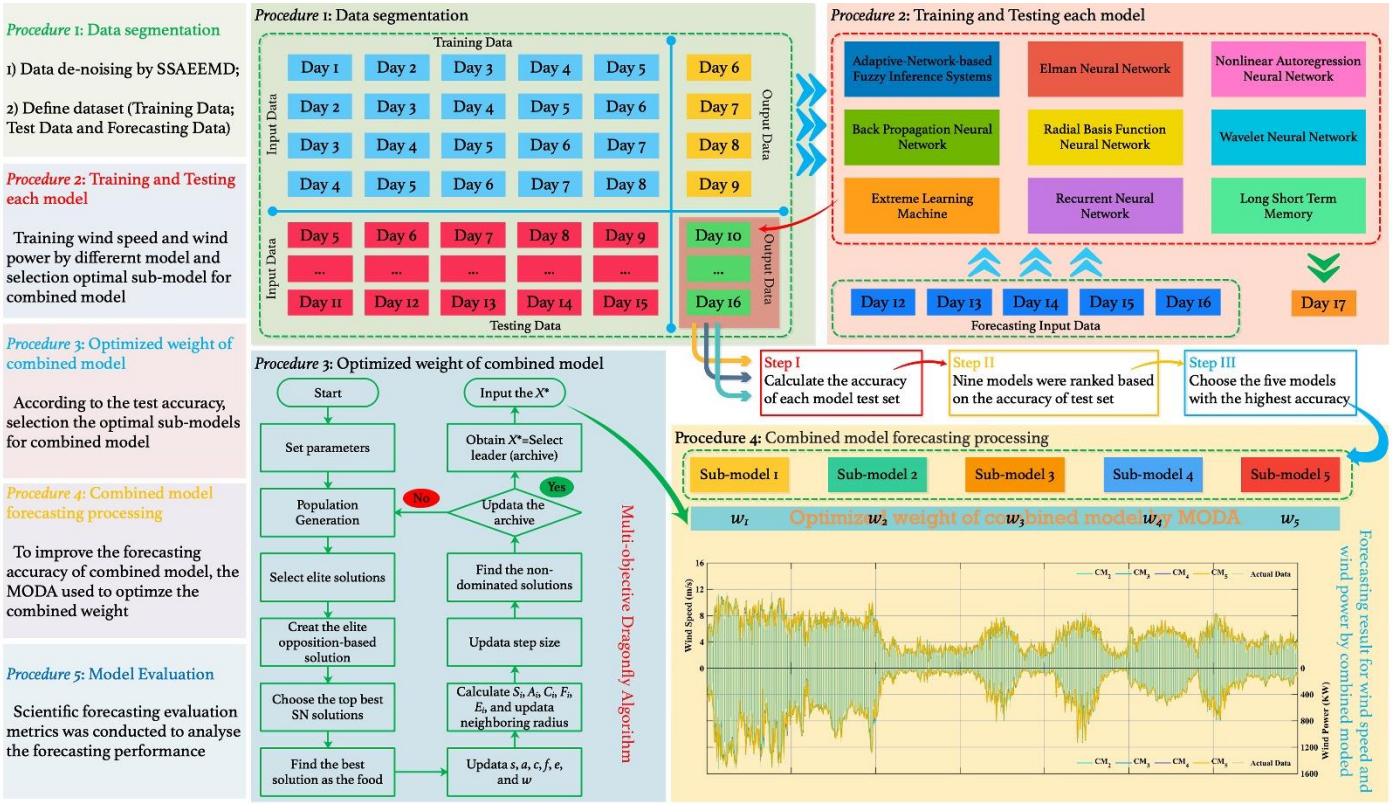

Figure 1. Flow Chart of the Proposed Model.

Procedure 1: Data Pretreatment

This stage included two integral parts. First, SSA was used to decompose the raw wind speed series into a (*r*) low-frequency components group [52] and a (*d*-*r*) high-frequency components group, according to KPAC. Second, EEMD [53] was utilized to further denoise the (*d*-*r*) high-frequency components group on the premise of SSA.

Procedure 2: Prediction of Hybrid Models

The forecasting accuracy of a single model cannot be optimal when a change in training data occurs during the forecasting process. Thus, single models do not always give optimal forecasting results when training data changes. To avoid a poor forecasting performance, combined models were developed. In this study, seven different models (ANFIS, BPNN, ELM, ENN, GRNN, LSTM, RNN, WNN and SVM) were employed to forecast wind speed and wind power, and five optimal forecasting models were selected as sub-models of the combined model. Meanwhile, data pre-processing was used to eliminate noise and useless information in the original time series. In the process of forecasting and modeling, the first 9 days (1296 data point) were used as the training set for the model, and days 10–14 (720 data points) were used as the testing set of the model. Each model produced 144 forecasting values.

Procedure 3: Establishment of the Proposed Combined System

After completing the modeling and forecasting process for the single hybrid model, the accuracy of each model testing set was calculated, and the five forecasting models with the highest accuracy levels were selected as sub-models of the combined model. Then, the testing data (720 data points) of the sub-models were used to build the combined model. The modified multi-objective dragonfly algorithm (the detail of MODA shown in Appendix A) was used to determine the optimal weight of the combined model. Subsequently, the forecasting results obtained from every individual model were integrated using the obtained weight coefficients, and wind speed and wind power forecasting was conducted.

Procedure 4: Wind Speed and Wind Power Forecasting

Based on realistic data, the developed combined model was used to carry out day-ahead forecasting. The theory behind day-ahead forecasting is as follows: First, the forecast origin and forecast horizon are set and denoted by a time point h and a positive whole number l, respectively. Then, if we want to forecast $\hat{y}_{h+l}$ at time point h where $l \geq 1$, we now define $\hat{y}_h(l)$ as the prediction data of y_{h+l}; therefore, $\hat{y}_h(l)$ can represent the l-step day-ahead forecasting of $\boldsymbol{y}_t$ at prediction point h. Once $l = 1$, $\hat{y}_h(l)$ is used to carry out one-step day-ahead forecasting [54].

Procedure 5: Model Evaluation

The forecasting precision and stability of the models during point forecasting were evaluated by four metrics. Three metrics were used for the uncertainty analysis.

3. Experiment and Results

In this section, the wind speed series data selection and experiment settings used for our study are illustrated systematically.

3.1. Data Acquisition

In this paper, the original wind speed and wind power time series used for forecasting were acquired in 2018 from four observation sites in Shandong province in China. These were used to establish and test the forecasting performance of each model.

Statistical descriptions for the datasets obtained for the two sites (mean, standard deviation, skewness, kurtosis, minimum, maximum, and median) are provided in Table 1. The mean values characterize the central tendency of the historical observations. The standard deviation values (the wind speed hovered around 2 m/s, and the wind power was around 200 kw) clearly reflect the fluctuations in wind speed and wind power. The skewness values of the wind speed and wind time series were greater than zero, which indicates that both types of time series had right-skewed distributions. Most wind time series had peak values greater than 3, indicating a fat tail distribution. Most kurtosis values of the wind power time series were greater than 3, indicating a fat tail distribution. The kurtosis values of the wind speed time series were less than 3, indicating a slight tail distribution.

Table 1. Statistical descriptions for wind speed and wind power.

Type	Period	Site	Mean	Standard Deviation	Skewness	Kurtosis	Minimum	Maximum	Median
Wind Power	1st season	Site 1	411.7689	363.5244	1.0921	3.5363	1.8000	1531.5000	306.4000
		Site 2	305.9613	321.8997	1.6886	5.5276	0.3000	1513.3000	183.2500
		Site 3	389.7726	365.3030	1.4564	4.3496	1.3000	1536.0000	258.8000
		Site 4	492.9215	393.0559	0.7732	**2.5640**	3.3000	1523.5000	385.3000
	2nd season	Site 1	489.9329	410.8507	0.7160	**2.3936**	3.3000	1526.0000	385.2500
		Site 2	265.8611	283.6276	2.0574	7.6069	1.8000	1525.5000	158.1500
		Site 3	434.1101	399.5205	1.2323	3.4904	2.5000	1540.5000	295.0500
		Site 4	564.8915	480.9706	0.5564	**1.8021**	10.5000	1531.5000	411.0000
	3rd season	Site 1	424.9078	381.9728	1.0105	3.0595	3.3000	1526.0000	291.0500
		Site 2	276.0506	292.7475	1.8652	6.5899	1.8000	1525.5000	153.9000
		Site 3	592.1482	446.7148	0.6088	**2.0907**	5.3000	1542.5000	456.8000
		Site 4	488.0642	390.1739	0.9079	3.0299	7.8000	1514.5000	398.3000
	4th season	Site 1	380.6880	324.9817	0.8102	**2.7174**	2.5000	1462.3000	277.6500
		Site 2	283.2654	280.0499	1.8746	6.5163	0.3000	1517.8000	179.5000
		Site 3	268.0734	230.0943	1.5841	5.9610	1.5000	1346.5000	195.9000
		Site 4	421.4685	345.8556	1.0779	3.4431	0.5000	1526.0000	326.9000
Wind Speed	1st season	Site 1	5.1481	2.2185	0.4563	**2.4600**	1.2000	11.6000	4.9000
		Site 2	4.5349	2.1664	0.9898	3.5858	1.4000	12.6000	4.0000
		Site 3	5.1488	2.2517	0.6968	**2.8510**	1.2000	12.0000	4.7000
		Site 4	5.8518	2.4114	0.3464	**2.3357**	1.0000	12.4000	5.6000
	2nd season	Site 1	4.9307	2.2821	0.3152	**2.0210**	1.1000	11.0000	4.7000
		Site 2	3.9232	1.7690	1.0834	3.9326	1.1000	10.5000	3.5000
		Site 3	4.8579	2.2117	0.6551	**2.9134**	1.0000	12.7000	4.5500
		Site 4	5.6659	2.6578	0.3630	**1.9376**	1.3000	11.8000	5.2500
	3rd season	Site 1	4.5910	1.9214	0.4164	**2.3272**	1.3000	10.3000	4.4000
		Site 2	4.0730	1.5074	0.7948	3.5370	1.3000	10.7000	3.8000
		Site 3	5.0499	1.8318	0.0851	**2.5125**	0.8000	10.4000	5.1000
		Site 4	6.0569	2.4137	0.0421	**2.1270**	1.0000	11.9000	6.0000
	4th season	Site 1	4.5007	1.8974	0.3944	**2.1300**	1.2000	9.8000	4.2000
		Site 2	4.1078	1.7622	1.2393	4.9165	1.0000	12.1000	3.7000
		Site 3	4.1116	1.5963	0.5948	**2.7939**	1.2000	9.7000	3.8000
		Site 4	4.8970	1.9637	0.4211	**2.5776**	0.8000	10.9000	4.7000

Note: Bold represents kurtosis values less than 3, indicating a slight tail distribution in the time series.

3.2. Experimental Setup

In this study, three experiments were conducted to verify the validity, superiority, and generalizability of the proposed combinatorial optimization model. Experiment I was designed to compare the forecasting performances of combined models with different numbers of sub-models for wind speed and wind power forecasting in the first season. Experiment II contrasted the forecasting performances of the combined models. The models were optimized by different optimization algorithms for wind speed and wind power forecasting in the second season. Experiment III verified the performance of the combined model for wind speed and wind energy forecasting in the third and fourth seasons. The details of the experiments are as follows:

Experiment I was designed to compare the combined model with different numbers of forecasting sub-models to determine the optimal number of sub models required by the combined model. Wind speed and wind power data collected from four sites in the first season were used to determine the forecasting capacity of the proposed model. Furthermore, the forecasting step was classified as day-ahead and used to assess the conducted models.

Experiment II was conducted to compare the performances of different optimization algorithms to optimize the weight of the combined model. Wind speed and wind power series from Site 1 to Site 4 in the second season were collected at 10 min intervals to establish four combined models based on different optimization algorithms.

Experiment III aimed to verify the applicability of the combined model based on five sub-models and optimized by MODA. Wind speed and wind power time series data collected at 10 min intervals in the third and fourth seasons were employed to verify the prediction performance of the combined model for day-ahead forecasting. Table 2 shows the forecasting precision and stability of the models during point forecasting.

Table 2. The forecasting metric for each model.

Metric	Definition	Equation
MAE	The mean absolute error of N forecasting results	$\mathrm{MAE} = \frac{1}{N}\sum_{n=1}^{N}\lvert y_n - \hat{y}_n\rvert$
RMSE	The root mean square error of N forecasting results	$\mathrm{RMSE} = \sqrt{\frac{1}{N}\sum_{n=1}^{N}(y_n - \hat{y}_n)^2}$
MAPE	The mean absolute percentage error of N forecasting results	$\mathrm{MAPE} = \frac{1}{N}\sum_{n=1}^{N}\frac{\lvert y_n-\hat{y}_n\rvert}{y_n}$
STD of APE	The standard deviation of absolute percentage error of N forecasting results	$\mathrm{STDAPE} = \sqrt{\mathrm{Var}\left(\frac{\lvert y_n-\hat{y}_n\rvert}{y_n}\right)}$
R^2	The goodness-of-forecasting fit	$R^2 = \frac{\sum_{n=1}^{N}(y_n-\overline{y})-\sum_{n=1}^{N}(y_n-\hat{y}_n)}{\sum_{n=1}^{N}(y_n-\overline{y})}$
DA	Directions or turning points between actual and forecasting values	$\mathrm{DA} = \frac{100}{N-1}\sum_{n=1}^{N-1} m_t$
U1	U-Statistic of 1-order	$\mathrm{U1} = \frac{\sqrt{\frac{1}{N}\sum_{n=1}^{N}(y_n-\hat{y}_n)^2}}{\sqrt{\frac{1}{N}\sum_{n=1}^{N}(y_n)^2}+\sqrt{\frac{1}{N}\sum_{n=1}^{N}(\hat{y}_n)^2}}$
U2	U-Statistic of 2-order	$\mathrm{U2} = \frac{\sqrt{\frac{1}{N}\sum_{n=1}^{N}\left(\frac{y_{n+1}-\hat{y}_{n+1}}{y_n}\right)^2}}{\sqrt{\frac{1}{N}\sum_{n=1}^{N}\left(\frac{y_{n+1}-\hat{y}_n}{y_n}\right)^2}}$

3.3. Performance Metrics and Benchmark Model

Five fitting error indices and two main benchmark models were introduced to ensure the predictability of the proposed model. These indicators were MAE, RMSE, MAPE, STDAPE, DA, U1, U2, and R^2 (the coefficient of determination), as well as seven ANN models. MAPE was a significant focus.

3.4. Parameter Setting

Parameter settings and initializations important to the methods applied included the following:

Input dimension. For the input vector, we set varying values of 1–8 for the input vector based on the ten-minute wind speed data and values of 1–6 for the input vector based on the 10-min wind power and wind speed data. The results of our empirical study indicated that the forecasting accuracy was at its best when the input vector dimension was 6.

SSA decomposition and EEMD denoising. For the previously mentioned SSA decomposition stage, the window length L and the principal components were the two most vital factors. On the basis of the trial-and-error method, $\boldsymbol{L}$ was set to 24 for ten-minute intervals to assess the wind speed transition and wind power from observation Sites 1 to Site 4 due to the homogeneity of the data structure among intervals. Thirteen principal components were selected for all sites. Table 3 shows the eigenvalue contributions to the various low- and high-frequency data groups in the time sequences. Taking the Site 1 wind speed series as an example, the principal components related to the first 13 eigenvalues accounted for 97.7643% of the variability, representing the main trend in the series. Further denoising was carried out for the high-frequency components. By parity of reasoning, the wind power time series data from the four sites were also analyzed by SSA using the trial-and-error and principal component analysis methods. The details are given in Table 3. For the EEMD

denoising stage, the number of IMFs was acquired by the formula $\log_2 N - 1$, where N is the length of the series. The IMFs ranged from high-frequency to low-frequency.

Table 3. Results for four sites after SSA.

Data Sets	Frequency	Site 1		Site 2	
		Eigenvalue	$\sum_{i=1}^{r}\lambda_i / \sum_{i=1}^{d}\lambda_i$	Eigenvalue	$\sum_{i=1}^{r}\lambda_i / \sum_{i=1}^{d}\lambda_i$
Wind Speed	Low	1–13	97.7643	1–13	95.5416
	High	14–24	2.2357	14–24	4.4584
Wind Power	Low	1–13	96.2804	1–13	95.5364
	High	14–24	3.7196	14–24	4.4636
Data Sets	**Frequency**	**Site 3**		**Site 4**	
		Eigenvalue	$\sum_{i=1}^{r}\lambda_i / \sum_{i=1}^{d}\lambda_i$	**Eigenvalue**	$\sum_{i=1}^{r}\lambda_i / \sum_{i=1}^{d}\lambda_i$
Wind Speed	Low	1–13	98.0989	1–13	99.1851
	High	14–24	1.9011	14–24	0.8149
Wind Power	Low	1–13	94.3994	1–13	92.8841
	High	14–24	5.6006	14–24	7.1159

For MODA, the population size of the dragonfly was 40, the archive size was 500, and the maximum number of iterations was 200.

For each artificial neural network, the building and training of the network were nearly parallel. There were 5 input layer neurons, 20 initial hidden layer neurons, and 1 output layer neuron.

3.5. Experimental Results and Analysis

This section presents the results from the three experiments on the forecasting performance of the proposed novel model.

3.5.1. Experiment I: The Forecasting Performance of the Combined Models Optimized by Different Optimization Algorithms

Based on the historical wind speed and wind power time series, four experiments were designed to analyze and contrast the developed combined model with the sub-model forecasting models. Experiment I contrasted combined models with different numbers of sub-models in terms of their forecasting performances and analyzed the ability of the proposed model with five sub-models to forecast wind speed and wind power. The wind speed and wind power forecasting performance were evaluated by eight metrics.

For Site 1, the proposed combined model had the best forecasting performance for both wind speed forecasting and wind power forecasting. Specifically, the mean absolute percentage error (MAPE) value was 6.51% for wind speed forecasting and 13.21% for wind power forecasting, smaller than those of the other combined models and sub-models. The relevant characteristics of the models used for Site 1 are shown in Figure 2.

For Site 2, the best mean absolute error (MAE), root-mean-square error (RMSE), mean absolute percentage error (MAPE), and standard deviation of absolute percentage error (STDAPE) were all obtained with the developed combined method for wind speed forecasting, with values of 0.2608, 0.3783, 6.90%, and 6.41%, respectively. For wind power forecasting, the best forecasting metrics were obtained with the proposed combined model shown in Table 4. This confirms the good performance of the proposed combined model.

Figure 2. Wind speed and wind power forecasting result in first season.

For Site 3, the wind speed forecasting accuracy of the combined model with five sub-models was significantly better than that of the combined models with less than five sub-models. This means that increasing the number of sub-models can improve the forecasting accuracy of the combined model.

The forecasting results of the combined model for Site 4 were similar to those obtained for previous sites; the proposed combined model provided better forecasting results in the first season. Taking wind power forecasting as an example, the lowest MAPE value, obtained with the advanced model, was 13.66%. The combined model with two sub-models had the worst forecasting result, having a MAPE value of 18.48% (the forecasting results of the sub-models are shown in Table A1). Table 4 also shows that the goodness of fit values for different combined models were over 0.9, indicating that combined models have a reduced forecasting error.

Table 4. Wind speed forecasting results for each site by different models for the first season.

Metric	Wind Speed Forecasting Result				Wind Power Forecasting Result			
	MODA-CM2	**MODA-CM3**	**MODA-CM4**	**MODA-CM5**	**MODA-CM2**	**MODA-CM3**	**MODA-CM4**	**MODA-CM5**
MAE	0.4062	0.3719	0.3354	0.3001	40.056	36.561	33.0686	29.6338
RMSE	0.5721	0.5251	0.4724	0.4235	72.7933	66.3983	59.9124	53.9345
STDAPE	9.23%	8.45%	7.62%	6.83%	51.54%	46.59%	42.60%	38.78%
DA	77.36%	79.44%	81.63%	83.32%	75.97%	78.15%	79.94%	81.93%
U1	0.051	0.0468	0.0421	0.0378	0.0664	0.0605	0.0546	0.0492
U2	0.9416	0.9313	0.9228	0.9166	0.7976	0.8011	0.8082	0.8168
MAPE	8.81%	8.06%	7.27%	6.51%	17.78%	16.21%	14.68%	13.21%
R^2	0.9663	0.9716	0.9771	0.9816	0.9798	0.9832	0.9863	0.9879
MAE	0.3524	0.3221	0.2917	0.2608	27.9611	25.4445	23.082	20.5847
RMSE	0.5098	0.4669	0.4234	0.3783	47.9482	43.5267	39.6267	35.2723
STDAPE	9.39%	8.57%	7.77%	6.90%	93.10%	85.07%	82.63%	71.73%
DA	78.05%	79.74%	82.03%	85.00%	75.47%	77.66%	79.05%	81.13%
U1	0.0508	0.0466	0.0422	0.0377	0.0542	0.0492	0.0448	0.0399
U2	0.9873	0.9719	0.9596	0.9502	0.9234	0.9301	0.9345	0.9415
MAPE	8.67%	7.93%	7.17%	6.41%	19.52%	17.81%	16.31%	14.49%
R^2	0.9719	0.9765	0.9807	0.9846	0.9888	0.9908	0.9924	0.994
MAE	0.4258	0.3881	0.3521	0.3145	42.9189	39.2509	35.4895	31.7399
RMSE	0.6075	0.5541	0.5036	0.4504	76.0106	69.6039	62.6796	56.1495
STDAPE	10.77%	9.83%	8.91%	7.97%	42.11%	40.08%	34.50%	32.30%
DA	78.15%	79.94%	81.63%	83.12%	77.56%	79.74%	81.63%	82.72%
U1	0.0541	0.0494	0.0449	0.0401	0.071	0.0651	0.0586	0.0525
U2	0.8735	0.8645	0.8654	0.8688	0.963	0.9666	0.9691	0.9719
MAPE	9.47%	8.63%	7.82%	7.00%	17.80%	16.32%	14.69%	13.21%
R^2	0.9629	0.9692	0.9747	0.9798	0.9783	0.9818	0.9852	0.9882
MAE	0.4195	0.3825	0.3466	0.3111	46.5028	42.4459	38.4124	34.4107
RMSE	0.6343	0.5784	0.5246	0.4716	82.4384	75.2224	68.0996	61.1102
STDAPE	12.47%	11.30%	10.26%	9.22%	66.74%	62.73%	55.86%	49.06%
DA	72.00%	72.79%	74.58%	75.87%	72.59%	73.09%	74.08%	75.07%
U1	0.0503	0.0459	0.0416	0.0374	0.0653	0.0596	0.054	0.0485
U2	0.952	0.9354	0.9269	0.9191	0.9773	0.9768	0.9758	0.9755
MAPE	8.31%	7.57%	6.86%	6.16%	18.48%	16.96%	15.26%	13.66%
R^2	0.9648	0.9708	0.9761	0.9808	0.9779	0.9816	0.9849	0.9879

Remark 1. *A general survey of the forecasting results for wind speed and wind power in the first season showed that the proposed combined model hds an optimal wind speed forecasting capacity. MAPE values at one day ahead were 6.51%, 6.41%, 7.00%, and 6.16% for Sites 1 to 4, respectively. Meanwhile, for wind power forecasting, the proposed combined model had the lowest forecasting error among all involved models. Moreover, for the forecasting results of wind speed and wind power, the MAPE value of wind power was twice that of wind speed with similar goodness-of-fit values.*

3.5.2. Experiment II: The Forecasting Performance of Combined Models Optimized by Different Optimization Algorithms

This experiment was designed to compare combined models optimized by different optimization algorithms, including MOGWO, MODA, MOMVO, and MODE. This experiment aimed to assess wind speed and wind energy forecasting in the second season. The evaluation metrics obtained for each model (MAE, RMSE, STDAPE, DA, U1, U2, MAPE and R^2) are shown in Table 5 and Figure 3.

For Site 1, the combined model optimized by MODA for wind speed forecasting and the combined model optimized by MODA for wind power forecasting produced the most accurate forecasting results in the most efficient manner. The MAPE values of the optimal combined model were 8.965% and 19.506%, respectively. In comparison, the forecasting performances of the combined models optimized by four algorithms showed no significant differences; for example, the RMSE values of the four combined models were 0.4647, 0.4649, 0.4644, and 0.4648 for wind speed forecasting. The wind power forecasting results for each model are listed in Table 5.

Table 5. Wind speed forecasting result for each site by different models in the second season.

Site	Data	Model	MAE	RMSE	STDAPE	DA	U1	U2	MAPE	R^2
Site 1	Wind speed	MOGWO-CM5	0.3533	0.4647	9.07%	78.55%	0.0457	0.7801	8.97%	0.9765
		MODA-CM5	0.3531	0.4644	9.06%	78.55%	0.0456	0.7798	8.97%	0.9765
		MOMVO-CM5	0.3533	0.4649	9.08%	78.45%	0.0457	0.7802	8.97%	0.9765
		MODE-CM5	0.3533	0.4648	9.08%	78.35%	0.0457	0.7799	8.97%	0.9765
	Wind power	MOGWO-CM5	36.8124	58.3834	61.35%	70.51%	0.0510	0.5874	19.52%	0.9883
		MODA-CM5	36.8083	58.3819	61.15%	70.51%	0.0511	0.5861	19.51%	0.9884
		MOMVO-CM5	36.8087	58.3822	61.58%	70.41%	0.0512	0.5862	19.54%	0.9883
		MODE-CM5	36.8282	58.3929	61.58%	70.31%	0.0511	0.5868	19.54%	0.9883
Site 2	Wind speed	MOGWO-CM5	0.3702	0.5147	11.57%	77.36%	0.0591	0.7825	10.41%	0.9599
		MODA-CM5	0.3701	0.5146	11.57%	77.36%	0.0591	0.7828	10.41%	0.9599
		MOMVO-CM5	0.3701	0.5147	11.58%	77.16%	0.0591	0.7826	10.41%	0.9599
		MODE-CM5	0.3702	0.5148	11.59%	77.46%	0.0592	0.7828	10.41%	0.9599
	Wind power	MOGWO-CM5	28.566	53.2864	37.05%	71.40%	0.0663	0.7942	17.77%	0.9833
		MODA-CM5	28.5521	53.2496	36.91%	71.40%	0.0662	0.7945	17.75%	0.9834
		MOMVO-CM5	28.5809	53.3471	37.05%	71.30%	0.0663	0.7949	17.77%	0.9833
		MODE-CM5	28.5791	53.3585	37.09%	71.40%	0.0664	0.7944	17.77%	0.9833
Site 3	Wind speed	MOGWO-CM5	0.5719	0.7595	13.09%	74.68%	0.063	0.7921	11.93%	0.9438
		MODA-CM5	0.5719	0.7595	13.08%	74.78%	0.063	0.7925	11.92%	0.9438
		MOMVO-CM5	0.572	0.7598	13.10%	74.88%	0.063	0.7931	11.93%	0.9437
		MODE-CM5	0.5723	0.7601	13.10%	74.58%	0.063	0.7923	11.93%	0.9437
	Wind power	MOGWO-CM5	67.6516	102.8315	55.22%	70.11%	0.0696	0.8788	21.67%	0.9731
		MODA-CM5	67.6172	102.7371	54.96%	70.31%	0.0695	0.8781	21.65%	0.9732
		MOMVO-CM5	67.6892	102.9403	55.08%	70.11%	0.0696	0.8776	21.68%	0.9731
		MODE-CM5	67.6626	102.8442	55.40%	70.21%	0.0696	0.8793	21.68%	0.9731
Site 4	Wind speed	MOGWO-CM5	0.4162	0.6063	10.78%	60.68%	0.0534	1.1342	8.88%	0.9623
		MODA-CM5	0.4162	0.6061	10.77%	60.58%	0.0534	1.134	8.88%	0.9624
		MOMVO-CM5	0.4164	0.6064	10.77%	60.68%	0.0534	1.1338	8.89%	0.9623
		MODE-CM5	0.4163	0.6063	10.77%	60.58%	0.0534	1.1338	8.89%	0.9623
	Wind power	MOGWO-CM5	45.4275	81.9936	24.61%	61.87%	0.0656	1.0822	14.23%	0.9777
		MODA-CM5	45.4039	81.9297	24.57%	61.77%	0.0656	1.0824	14.23%	0.9778
		MOMVO-CM5	45.4503	82.1035	24.63%	61.87%	0.0657	1.0824	14.23%	0.9777
		MODE-CM5	45.4691	82.0945	24.64%	61.77%	0.0657	1.0824	14.24%	0.9777

For wind speed forecasting at Site 2, the combined model optimized by MODA obtained the best assessment metrics for wind speed forecasting. Specifically, for wind speed forecasting, the MAPE value obtained by the combined model optimized by MOGWO was 10.409%, better than the values obtained by the combined models optimized by MOGWO, MOMVO, and MODE by 0.0019%, 0.0019%, and 0.0048%. These models were ranked from second to last in terms of their forecasting accuracy, respectively. Figure 3 shows the wind power forecasting results for the combined models optimized by four optimization algorithms.

For Site 3, all of the combined models optimized by optimization algorithms provided satisfactory wind speed and wind power forecasting results, as proven by their better goodness-of-fit values compared with those of the sub-models (the forecasting results of sub-models shows in Table A2).

For Site 4, the combined models optimized by four different optimization algorithms showed outstanding forecasting potential. For wind power forecasting, the combined model optimized by MODA obtained the lowest MAE, RMSE, STDAPE, and MAPE values of 45.4039, 81.9297, 24.57%, and 14.226%, respectively. There were no obvious differences in MAPE among the other combined models.

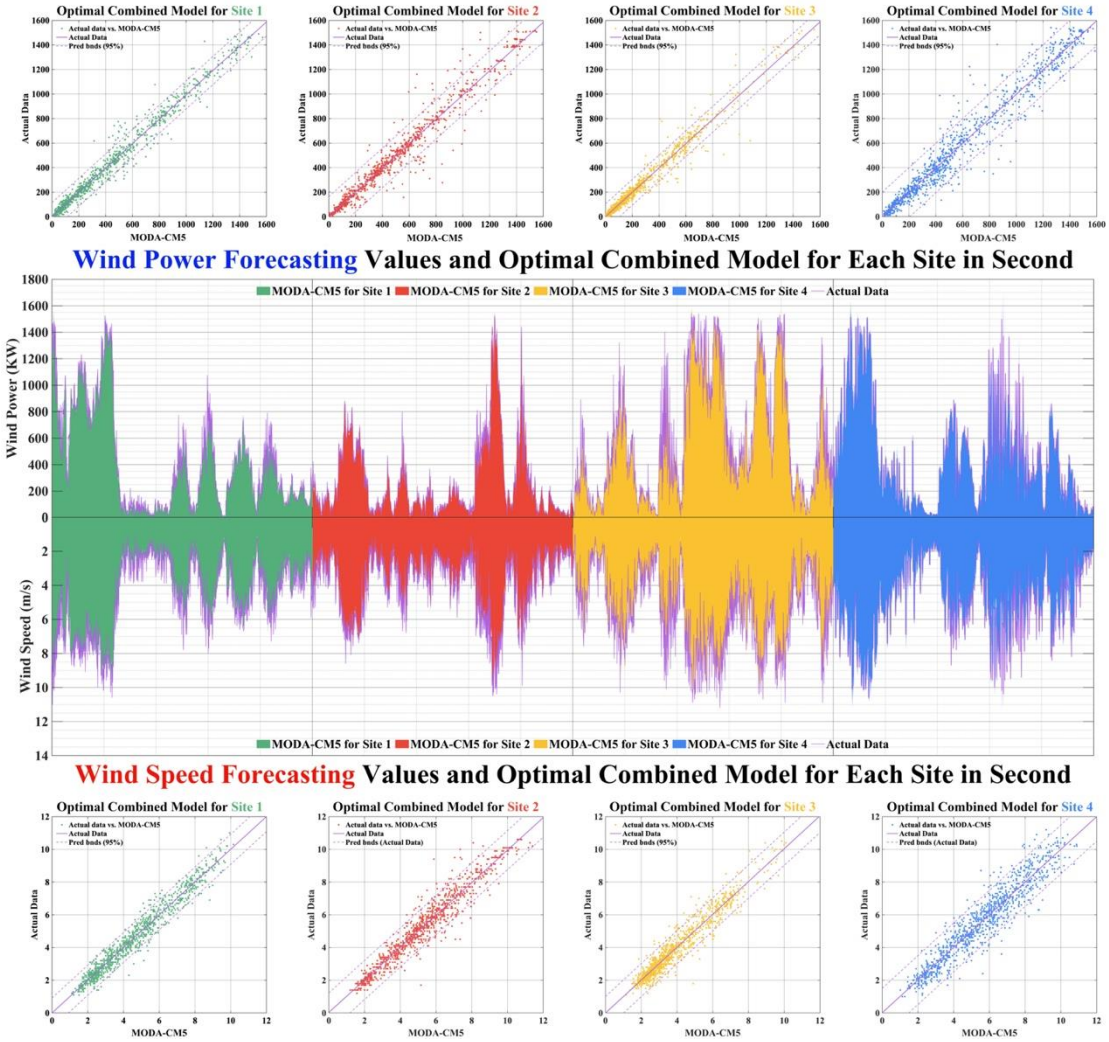

Figure 3. The optimal combined model for wind power and wind speed forecasting.

Remark 2. *The evaluation index values obtained in Experiment II reveal that regardless of the optimization algorithm applied to optimize the combined model and the site used for forecasting, there is no optimal method for wind speed and wind power forecasting. For the second season of wind speed and wind power forecasting, the forecasting evaluation metrics of the combined models optimized by each algorithm had no significant differences.*

3.5.3. Experiment III: Verification of the Performance of the Combined Model Based on Five Sub-Models and Optimized by MODA

In this experiment, 10 min intervals of wind speed and wind power forecasts in the third and fourth seasons were analyzed. The forecasting results for wind speed and wind power at four observation sites are shown in Figures 4 and 5, and the forecasting performance of each model, as evaluated by eight metrics, is shown in Tables 6 and 7. The results illustrate the following:

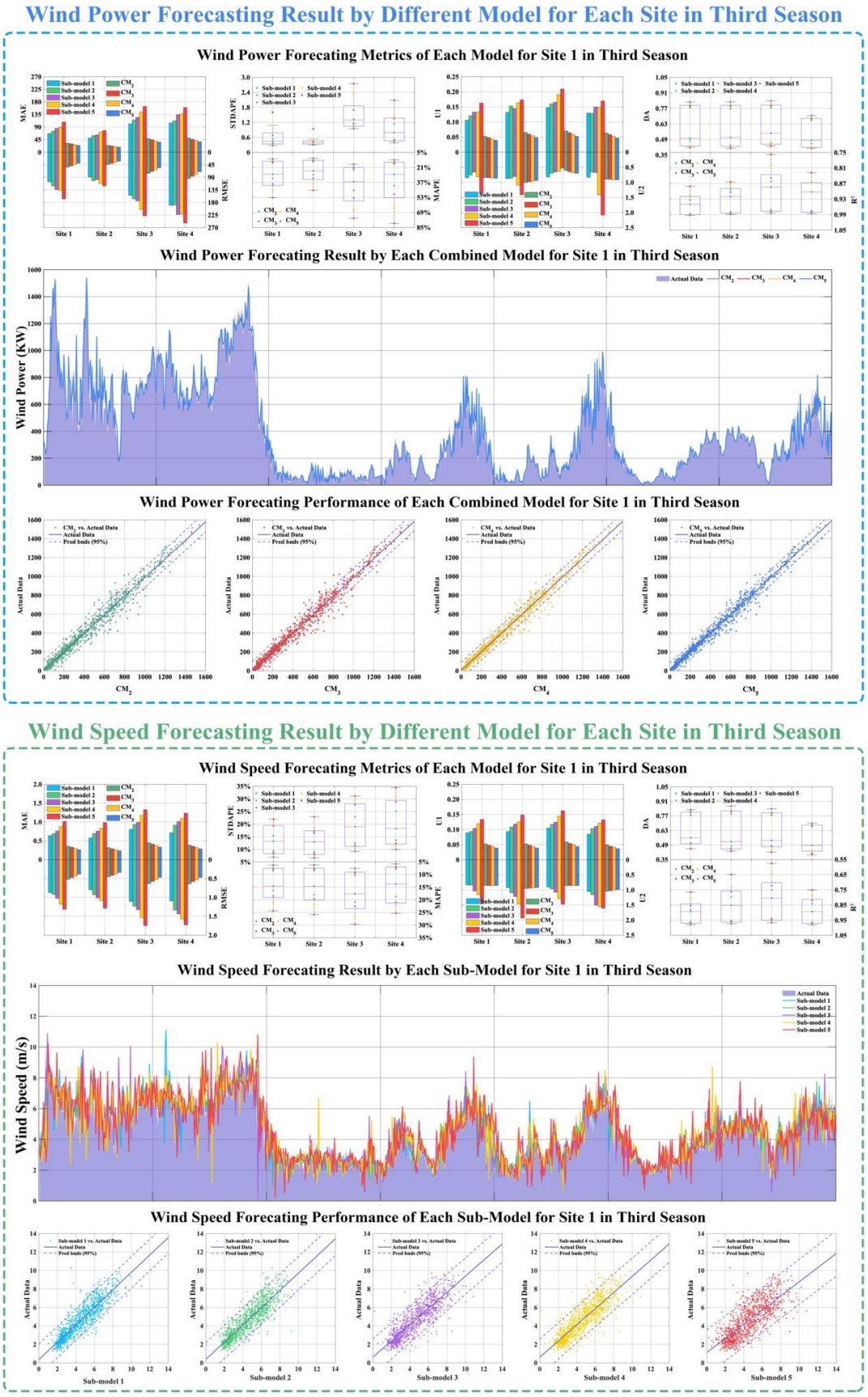

Figure 4. Wind speed and wind power forecasting result for each site in the third season.

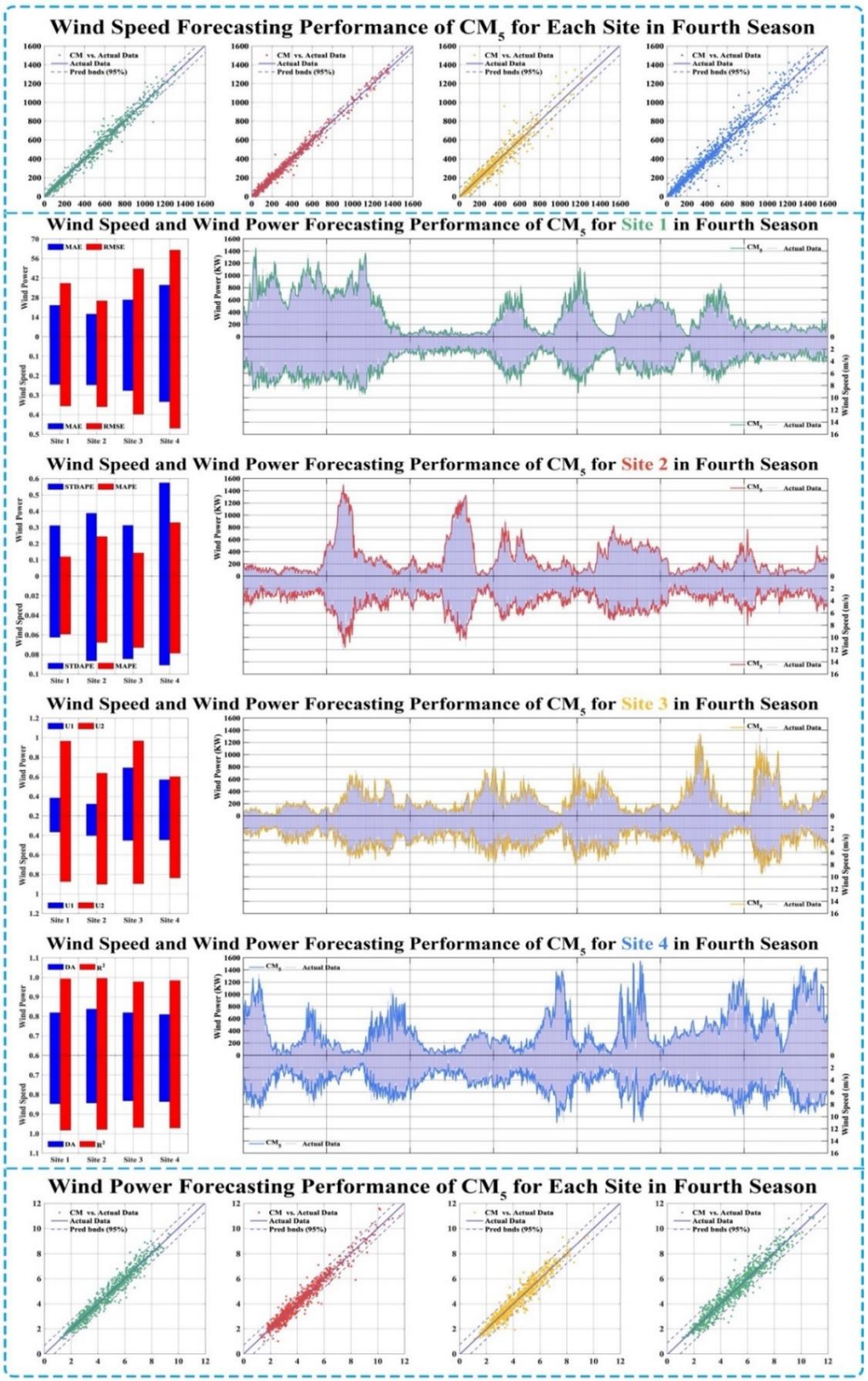

Figure 5. Wind speed and wind power forecasting result for each site by the CM5 model.

Table 6. The forecasting result of wind speed and wind power in the third season.

Site	Model	Wind Speed Forecasting Result							
		MAE	RMSE	STDAPE	DA	U1	U2	MAPE	R^2
Site 1	MODA-CM2	0.3616	0.5242	9.37%	77.66%	0.0527	0.8608	8.50%	0.9622
	MODA-CM3	0.3299	0.4789	8.64%	80.24%	0.0482	0.8546	7.76%	0.9685
	MODA-CM4	0.2977	0.4301	7.79%	81.73%	0.0433	0.8564	7.01%	0.9746
	MODA-CM5	0.2676	0.3874	6.88%	82.82%	0.039	0.8577	6.29%	0.9795
Site 2	MODA-CM2	0.3204	0.4572	8.92%	78.85%	0.0527	0.9545	8.45%	0.9531
	MODA-CM3	0.2926	0.417	8.16%	81.43%	0.0481	0.94	7.72%	0.961
	MODA-CM4	0.2652	0.3791	7.48%	83.52%	0.0437	0.9312	7.00%	0.9678
	MODA-CM5	0.2365	0.3379	6.63%	86.00%	0.0389	0.9242	6.24%	0.9745
Site 3	MODA-CM2	0.4522	0.6379	12.53%	77.56%	0.0594	0.8627	10.26%	0.9376
	MODA-CM3	0.4115	0.5791	11.40%	79.64%	0.0539	0.8583	9.33%	0.9488
	MODA-CM4	0.3716	0.5228	10.32%	81.13%	0.0487	0.8561	8.43%	0.9585
	MODA-CM5	0.3336	0.4706	9.27%	83.22%	0.0438	0.8584	7.57%	0.9665
Site 4	MODA-CM2	0.3883	0.6405	13.61%	66.93%	0.0492	1.0477	7.92%	0.9643
	MODA-CM3	0.3547	0.5851	12.41%	67.73%	0.045	1.0224	7.22%	0.9702
	MODA-CM4	0.3205	0.5301	11.18%	69.02%	0.0407	1.0012	6.53%	0.9756
	MODA-CM5	0.2871	0.4752	10.18%	70.51%	0.0365	0.9905	5.86%	0.9804
Site	**Model**	**Wind Power Forecasting Result**							
Site 1	MODA-CM2	32.4895	53.7871	36.59%	77.86%	0.0525	0.8427	16.20%	0.9874
	MODA-CM3	29.6887	49.3502	33.95%	79.25%	0.0482	0.8462	14.83%	0.9894
	MODA-CM4	26.8511	44.4808	30.78%	80.93%	0.0435	0.854	13.46%	0.9913
	MODA-CM5	24.1056	40.1238	27.06%	82.72%	0.0392	0.8654	12.00%	0.9929
Site 2	MODA-CM2	24.2458	44.4954	43.91%	76.76%	0.0652	1.0144	14.99%	0.9802
	MODA-CM3	22.1599	40.7036	40.24%	79.15%	0.0596	0.9834	13.72%	0.9834
	MODA-CM4	20.055	36.9844	36.29%	81.13%	0.0542	0.9624	12.38%	0.9863
	MODA-CM5	17.9601	32.9801	31.82%	82.82%	0.0483	0.9421	11.10%	0.9891
Site 3	MODA-CM2	48.8722	76.0633	129.59%	77.56%	0.0708	0.612	23.75%	0.9717
	MODA-CM3	44.5428	69.2187	115.33%	79.44%	0.0644	0.6482	21.44%	0.9766
	MODA-CM4	40.3523	62.7414	101.21%	81.53%	0.0584	0.6876	19.35%	0.9808
	MODA-CM5	36.0848	56.0705	94.94%	83.71%	0.0522	0.7036	17.50%	0.9847
Site 4	MODA-CM2	50.3663	94.3956	51.41%	66.34%	0.0634	0.8965	17.36%	0.9760
	MODA-CM3	45.9655	86.1728	46.87%	67.73%	0.0579	0.901	15.87%	0.9788
	MODA-CM4	41.6598	78.4007	43.20%	68.82%	0.0527	0.9131	14.42%	0.9835
	MODA-CM5	37.2738	69.8088	38.74%	70.51%	0.0469	0.9179	12.92%	0.9865

(1) The combined model with five sub-models produced the smallest MAE, RMSE, STDAPE, U1, U2, and MAPE values and the largest DA and R^2 values at all sites. This indicates that the combined model has the best forecasting performance and stability.

(2) For wind power forecasting, the results of the combined model with five sub-models (CM5) for four sites, as evaluated by eight metrics, were better than those of the other combined models. For example, the RMSE values of the CM5 model at the four sites were 40.1238, 32.9801, 56.0705, and 69.8088. Compared with the other combined models, the forecasting accuracy of the CM5 was greater. The main reason for this is that the CM5 can effectively use the advantages of each sub-model and the weight of the combined model optimized by the optimization algorithm. By comparing the CM5 with the CM2, CM3 and CM4 models, we determined that the number of sub-models included influences the forecasting performance of the combined model. The MAPE value of the CM5 was 12.00% lower than those of the other combined models for Site 1 in the third season.

(3) For wind speed forecasting, the combined model obtained satisfactory forecasting results. The forecasting results of the combined models were better than those of the sub-models. Thus, the use of combined models can improve forecasting accuracy. For wind speed forecasting at Site 1, the MAPE values of the five sub-models were 14.61%, 16.31%, 18.46%, 21.04%, and 24.38%, respectively. In contrast, the MAPE value of the combined model (CM5) was 6.29%, an improvement of 8.32%, 10.02%, 12.17%, 14.75%, and 18.09%, respectively, compared with the five sub-models.

(4) The models' goodness of fit results are shown in Table 6. The minimum value was 0.9665, which proves that the forecasting series obtained by combined model (CM5) was consistent with the actual series.

Table 7. The forecasting results of each combined models for different sites in the fourth season.

Site	Model	Wind Speed Forecasting Result							
		MAE	RMSE	STDAPE	DA	U1	U2	MAPE	R^2
Site 1	MODA-CM2	0.3336	0.4826	8.47%	77.86%	0.0495	0.88	8.04%	0.9671
	MODA-CM3	0.3038	0.4388	7.71%	79.54%	0.045	0.8761	7.33%	0.9729
	MODA-CM4	0.2747	0.3969	6.98%	82.42%	0.0407	0.8736	6.63%	0.9779
	MODA-CM5	0.2455	0.3551	6.24%	84.71%	0.0364	0.8735	5.92%	0.9823
Site 2	MODA-CM2	0.3347	0.4866	11.57%	77.66%	0.0546	0.935	9.16%	0.9612
	MODA-CM3	0.3053	0.444	10.84%	79.74%	0.0498	0.922	8.38%	0.9677
	MODA-CM4	0.2761	0.4001	9.56%	82.03%	0.0449	0.9077	7.57%	0.9739
	MODA-CM5	0.2468	0.3549	8.65%	84.31%	0.0403	0.9007	6.77%	0.9789
Site 3	MODA-CM2	0.3734	0.5373	11.29%	79.34%	0.0609	0.9129	9.84%	0.9419
	MODA-CM3	0.3408	0.4907	10.26%	80.34%	0.0556	0.9039	8.98%	0.9517
	MODA-CM4	0.3086	0.4441	9.27%	81.83%	0.0504	0.8955	8.13%	0.9606
	MODA-CM5	0.2762	0.3978	8.44%	83.22%	0.0451	0.8951	7.29%	0.9685
Site 4	MODA-CM2	0.4509	0.6336	12.34%	77.66%	0.0604	0.8293	10.65%	0.9465
	MODA-CM3	0.4107	0.5774	11.26%	80.04%	0.055	0.8293	9.70%	0.9558
	MODA-CM4	0.3728	0.5245	10.22%	81.73%	0.05	0.8329	8.79%	0.9636
	MODA-CM5	0.3334	0.4693	9.09%	83.61%	0.0447	0.8365	7.86%	0.9711
Site	**Model**	**Wind Power Forecasting Result**							
Site 1	MODA-CM2	30.4507	51.8389	43.30%	76.86%	0.0519	0.9746	16.11%	0.9872
	MODA-CM3	27.7441	47.0719	38.51%	79.15%	0.0472	0.9691	14.64%	0.9895
	MODA-CM4	25.1217	42.7923	35.70%	80.64%	0.0429	0.9664	13.30%	0.9913
	MODA-CM5	22.4712	38.2385	31.23%	81.83%	0.0383	0.9648	11.87%	0.9931
Site 2	MODA-CM2	22.0638	35.0959	538.95%	78.25%	0.044	0.5185	33.41%	0.9922
	MODA-CM3	20.1148	31.8624	469.76%	80.54%	0.0399	0.5708	29.73%	0.9935
	MODA-CM4	18.1789	28.8482	451.01%	82.42%	0.0362	0.5857	27.77%	0.9947
	MODA-CM5	16.2631	25.6994	387.20%	83.71%	0.0322	0.6368	24.37%	0.9958
Site 3	MODA-CM2	35.7497	65.9754	42.12%	74.48%	0.0939	0.9555	19.27%	0.9581
	MODA-CM3	32.6873	60.0973	38.53%	77.76%	0.0856	0.9589	17.61%	0.9653
	MODA-CM4	29.6624	54.9203	34.63%	79.54%	0.0782	0.9615	15.93%	0.9711
	MODA-CM5	26.4136	48.6081	31.34%	81.83%	0.0692	0.9668	14.28%	0.9774
Site 4	MODA-CM2	50.0333	83.8969	749.01%	76.17%	0.0772	0.7179	43.81%	0.9702
	MODA-CM3	45.6821	76.5383	716.34%	77.46%	0.0704	0.6871	41.01%	0.9752
	MODA-CM4	41.1558	68.8028	626.17%	79.15%	0.0633	0.623	36.33%	0.9789
	MODA-CM5	36.9947	62.0098	574.43%	80.93%	0.0571	0.6016	33.05%	0.9838

Remark 3. *The CM5 combined model had the smallest MAE, RMSE, STDAPE, U1, U2, and MAPE values and the biggest R^2 and DA values. This indicates that combined models can identify changes in wind speed and wind power.*

To verify the applicability of the combined model with five sub-models optimized by MODA for determining the wind speed and wind power series, the forecasting results for the fourth season are shown in Table 7 and Figure 5.

For Site 1, in the fourth season, the combined model with five sub-models (CM5) obtained the best forecasting accuracy. For wind speed and wind power forecasting, the evaluation metrics of the CM5 were also better than those of combined models with less than five sub-models and for the sub-models individually. This means that the CM5 is more suitable for wind speed and wind power forecasting.

For Site 2, the sub-models and combined models showed analogical forecasting abilities in terms of the values obtained for the forecasting evaluation metrics. To be more specific, for wind speed forecasting, the MAPE values of the five sub-models were 16.30%, 18.64%, 20.90%, 23.90% and 27.26%, respectively. In contrast, the MAPE value of the combined model (CM5) was 6.77%—an improvement of 9.53%, 11.87%, 14.13%, 17.13%, and 20.49%, respectively, compared with the five sub-models (shown in Table A4).

As for Site 3, the combined model with five sub-models showed a superior performance to the other combined models based on the eight employed evaluation criteria with MAE, RMSE, STDAPE, DA, U1, U2, MAPE, and R^2 values for wind power forecasting of 26.4136, 48.6081, 31.34%, 81.83%, 0.0692, 0.9668, 14.28% and 0.9774, respectively. Among the remaining combined models, the ranking of methods in terms of their forecasting accuracy, from good to bad, was CM2, CM3, and CM4, with MAPE values of 19.27%, 17.61%, and 15.93%, respectively.

For Site 4, the MAPE values of the combined model (CM5) for wind speed and wind power forecasting were 7.86% and 33.05%, respectively. Compared with the other three combined models with the highest MAPE values, the combined model with five sub-models improved wind speed and wind power forecasting by 2.79% and 10.76%, respectively. Comparing the combined models and sub-models, the forecasting accuracy of the combined models was better. A comparison of the wind speed and wind power forecasting results for Site 4 is presented in Figure 5.

Remark 4. *The differences in the forecasting results obtained by the developed model and those obtained by the other individual models were significant. The evaluation indicator values obtained with the proposed model were more satisfactory, as they were lower than those computed with the contrasting models, regardless of the forecasting step. Hence, we conclude that the advanced combined model has a superior capacity relative to conventional individual models for short-term wind speed forecasting.*

4. Discussion

In this subsection, a comprehensive discussion related to the proposed model is provided. This includes two parts: a significance test for forecasting values and forecasting errors and a forecasting uncertainty analysis.

4.1. Significance Test between Forecasting Values and Actual Data

To evaluate the significance level of forecasting errors between the proposed combined model and the other models, a classical hypothesis test method, the Diebold–Mariano Test [55], was used to measure the significance of prediction errors for different models. Theoretical support for this model is as follows.

Given a certain probability of coming to a wrong conclusion α, the original hypothesis H_0 will not be rejected as long as the forecasting capacity of the proposed model possesses no evident distinction when contrasted with the comparison model; if the inverse is true, H_0 will be rejected and H_1 accepted. The hypothetical form is:

$$\begin{array}{l} H_0 : E[L(error^1)] = E[L(error^2)] \\ H_1 : E[L(error^1)] \neq E[L(error^2)] \end{array} \quad (1)$$

where L represents the loss function for forecasting errors, and $error^1$ and $error^2$ are the forecasting errors of the combined model with five sub-models and those of other combined models and single models, respectively.

Further, the DM statistical magnitude can be expressed by:

$$\mathrm{DM} = \frac{\sum_{i=1}^{n} \left(L(error^1) - L(error^2)\right)/n}{\sqrt{S^2/n}} \mathbf{s}^2 \quad (2)$$

In the above equation, S^2 is the estimated variance of $\mathbf{d} = L(error^1) - L(error^2)$.

After obtaining the calculated DM value, a comparison between the DM statistics and a critical value $Z_{\alpha/2}$ is conducted. Once the DM statistic is greater than $Z_{\alpha/2}$ or less than $-Z_{\alpha/2}$, the original hypothesis will be rejected. Moreover, it may be concluded that there is an evident distinction between our developed model and the compared model.

The Wilcoxon rank-sum test [56,57] is a nonparametric test that can be used to determine whether two independent samples have been selected from populations with the same distribution.

If $h = 1$, the null hypothesis that there is no difference between two samples at the 5% significance level is rejected.

If $h = 0$, there is a failure to reject the null hypothesis at the 5% significance level.

The results of the Diebold–Mariano test and Wilcoxon rank-sum test for wind speed and wind power forecasting are shown in Table 8. The following conclusions were made: First, the test results of DM test for wind speed showed little variation in the forecasting error among the different combined models, and the Wilcoxon rank-sum test results showed

no difference between the forecasting results of each model and the actual wind speed at the 5% significance level. When the combined models were compared, the combined model with five sub-models was found to be evidently different from the other models at the 1% significance level for wind power forecasting. However, the DM test between the combined model and the sub-model revealed that some sub-models obtained DM values that were higher than the threshold at a 5% significance level. For example, in the first season, the SSAWD-Elman sub-model had a DM value of 1.6448 for wind power forecasting. The test results for the other sub-models are shown in Table A5. The Wilcoxon rank-sum test result of each combined model showed no differences between the actual wind power values and the forecasting results of each combined model. Meanwhile, the Wilcoxon rank-sum test results presented in Table A5 show that some sub-models rejected the null hypothesis at the 5% significance level, which indicates that the forecasting results of some sub-models differed from the actual data.

Table 8. The results of the DM test and WRS test for wind speed and wind power by each combined model.

Period	Site	Test	Wind Speed				Wind Power			
			MODA-CM2	MODA-CM3	MODA-CM4	MODA-CM5	MODA-CM2	MODA-CM3	MODA-CM4	MODA-CM5
First Season	Site 1	DM Test	15.5146 *	14.8602 *	12.4159 *	-	8.5860 *	8.6528 *	6.6730 *	-
		WRS Test	0.696 (1)	0.6998 (1)	0.7299 (1)	0.7249 (1)	0.6832 (1)	0.6988 (1)	0.7095 (1)	0.7203 (1)
	Site 2	DM Test	13.1674 *	11.5685 *	10.0139 *	-	10.0496 *	9.5269 *	7.9863 *	-
		WRS Test	0.8018 (1)	0.7791 (1)	0.7916 (1)	0.7953 (1)	0.8747 (1)	0.8722 (1)	0.8702 (1)	0.8683 (1)
	Site 3	DM Test	14.0858 *	13.7322 *	13.5449 *	-	8.2746 *	8.6871 *	9.6449 *	-
		WRS Test	0.6724 (1)	0.6695 (1)	0.6935 (1)	0.7111 (1)	0.6688 (1)	0.6717 (1)	0.6756 (1)	0.6817 (1)
	Site 4	DM Test	12.2121 *	12.2736 *	10.0069 *	-	9.9215 *	9.8950 *	8.2886 *	-
		WRS Test	0.9969 (1)	0.9902 (1)	0.974 (1)	0.9904 (1)	0.8323 (1)	0.8339 (1)	0.8323 (1)	0.8319 (1)
Seconds Season	Site 1	DM Test	18.1848 *	16.5849 *	15.0379 *	-	11.2257 *	11.2726 *	10.0365 *	-
		WRS Test	0.8078 (1)	0.8047 (1)	0.8094 (1)	0.8068 (1)	0.8876 (1)	0.878 (1)	0.8706 (1)	0.8809 (1)
	Site 2	DM Test	13.8823 *	15.1337 *	12.4642 *	-	7.0921 *	6.4662 *	7.3349 *	-
		WRS Test	0.7429 (1)	0.7476 (1)	0.759 (1)	0.7608 (1)	0.7528 (1)	0.7378 (1)	0.7216 (1)	0.7325 (1)
	Site 3	DM Test	17.6655 *	16.8552 *	14.6886 *	-	11.4051 *	12.2241 *	9.1368 *	-
		WRS Test	0.5999 (1)	0.6083 (1)	0.613 (1)	0.6217 (1)	0.9473 (1)	0.942 (1)	0.9438 (1)	0.9398 (1)
	Site 4	DM Test	12.3603 *	13.1989 *	10.3810 *	-	8.9026 *	8.8885 *	8.0601 *	-
		WRS Test	0.7159 (1)	0.706 (1)	0.6962 (1)	0.7048 (1)	0.831 (1)	0.8319 (1)	0.8204 (1)	0.8272 (1)
Third Season	Site 1	DM Test	10.2836 *	10.0742 *	8.1850 *	-	10.4397 *	10.0330 *	7.9945 *	-
		WRS Test	0.8255 (1)	0.8297 (1)	0.8435 (1)	0.8549 (1)	0.9071 (1)	0.8986 (1)	0.8983 (1)	0.8945 (1)
	Site 2	DM Test	12.8066 *	14.1692 *	9.9269 *	-	5.8617 *	5.7684 *	7.1332 *	-
		WRS Test	0.8133 (1)	0.8018 (1)	0.7958 (1)	0.8084 (1)	0.9597 (1)	0.9449 (1)	0.9404 (1)	0.9437 (1)
	Site 3	DM Test	14.2602 *	14.8542 *	12.3259 *	-	12.5005 *	12.1284 *	10.7953 *	-
		WRS Test	0.6149 (1)	0.6449 (1)	0.647 (1)	0.666 (1)	0.6954 (1)	0.7037 (1)	0.707 (1)	0.7183 (1)
	Site 4	DM Test	9.8375 *	9.9908 *	9.1350 *	-	9.0853 *	8.9344 *	7.4904 *	-
		WRS Test	0.9427 (1)	0.966 (1)	0.9616 (1)	0.9752 (1)	0.9713 (1)	0.9665 (1)	0.9513 (1)	0.9471 (1)
Four Season	Site 1	DM Test	14.1478 *	13.6951 *	12.2685 *	-	8.9806 *	9.8720 *	7.0639 *	-
		WRS Test	0.9448 (1)	0.914 (1)	0.9242 (1)	0.9258 (1)	0.8697 (1)	0.8692 (1)	0.8744 (1)	0.8766 (1)
	Site 2	DM Test	11.9130 *	11.7688 *	9.2459 *	-	8.5189 *	8.9237 *	6.2209 *	-
		WRS Test	0.8767 (1)	0.8775 (1)	0.8527 (1)	0.8533 (1)	0.905 (1)	0.9045 (1)	0.8972 (1)	0.8991 (1)
	Site 3	DM Test	13.8255 *	13.7087 *	11.2639 *	-	7.2845 *	7.2283 *	7.4506 *	-
		WRS Test	0.4918 (1)	0.5037 (1)	0.5219 (1)	0.5325 (1)	0.7759 (1)	0.7637 (1)	0.7568 (1)	0.7548 (1)
	Site 4	DM Test	15.4436 *	15.1429 *	12.2494 *	-	10.0481 *	10.1940 *	9.0470 *	-
		WRS Test	0.947 (1)	0.9459 (1)	0.9562 (1)	0.9734 (1)	0.9623 (1)	0.9382 (1)	0.9193 (1)	0.9152 (1)

Note: * is the 5% significance level. (0) there is difference between two sample at the 5% significance level. (1) there is no dif-ference between two sample at the 5% significance level.

For the wind speed and wind energy forecasting error test results, there was little variation among the combined models at the 1% significance level, while there were greater differences between the combined models and the sub-models. Comparing the actual data with those forecast by each model, it was found that the wind speed data forecast by each sub-model and the real data represented the same sample at the 5% significance level. However, when the wind power forecasting values obtained with each model and the actual data were compared with the Wilcoxon rank-sum test result, they were found to represent two different samples at the 5% significance level. Based on these results, the wind speed forecasting accuracy was deemed to be higher than the wind power forecasting accuracy.

4.2. Uncertainty Analysis

Uncertainties in wind speed and wind power forecasting result in an imbalance between projected and actual time series, and this influences the operation reliability of wind farms [58]. Based on the forecasting results of a combined model for wind speed and wind power, interval forecasting was employed to analyze the level of uncertainty in wind speed and wind power forecasting and to assess possible threats for decision planners in terms of power dispatching.

More specifically, the uncertainty analysis used interval forecasting to analyze wind speed and wind power data sets from four seasons, each with a span of 10 min. By comparing the forecasting performances of different combined models and sub-models, the forecasting error of each model was analyzed in four seasons, and the differences in the prediction error were compared with the level of error in the proposed models, namely, the sub-model based on the ANN and the MODA-based combined model with different numbers of sub-models. Sub-models and combined models were used as contrasting models to verify the superiority of the proposed combined model in terms of interval forecasting. If the evaluation results of the proposed combined model were better than those of all comparison models under the same conditions, this would verify that the proposed model is better than combined models with less than five sub-models or sub-models alone in terms of uncertainty forecasting and stability forecasting [59].

To better identify the characteristics of the wind speed and wind power forecasting values from each model, a diverse probability density function including the *t* location-scale, stable distribution, logistic, and normal distribution functions was employed to fit the forecasting wind speed series and wind power series via maximum likelihood estimation (MLE) [60]. Referring to the results of the assessment index R^2 shown in Table 9 and Figure 6, the *t*-location scale and stable function was selected as the most suitable probabilistic distribution for further interval forecasting.

Table 9. R^2 Values of Each Distribution Fitting.

Model	Distribution	R^2 for Wind Speed				R^2 for Wind Power			
		Site 1	Site 2	Site 3	Site 4	Site 1	Site 2	Site 3	Site 4
MODA-CM2	Normal	0.8899	0.8770	0.8731	0.7568	0.6571	0.6800	0.6008	0.5499
	Logistic	0.9555	0.9487	0.9432	0.8549	0.8105	0.8522	0.7496	0.7045
	Stable	0.9760	0.9729	0.9671	0.9407	0.9795	0.9911	0.9698	0.9684
	t-Location Scale	0.9846	0.9825	0.9768	0.9466	0.9784	0.9926	0.9634	0.9573
MODA-CM3	Normal	0.8918	0.8752	0.8776	0.7670	0.6598	0.6813	0.6005	0.5572
	Logistic	0.9564	0.9468	0.9470	0.8650	0.8131	0.8529	0.7498	0.7132
	Stable	0.9761	0.9710	0.9704	0.9487	0.9831	0.9917	0.9694	0.9749
	t-Location Scale	0.9839	0.9812	0.9796	0.9544	0.9820	0.9933	0.9632	0.9642
MODA-CM4	Normal	0.8938	0.8766	0.8778	0.7755	0.6639	0.6822	0.6042	0.5599
	Logistic	0.9579	0.9490	0.9473	0.8739	0.8175	0.8563	0.7545	0.7160
	Stable	0.9772	0.9738	0.9708	0.9568	0.9848	0.9943	0.9726	0.9776
	t-Location Scale	0.9851	0.9839	0.9799	0.9624	0.9838	0.9953	0.9666	0.9682
MODA-CM5	Normal	0.8931	0.8766	0.8792	0.7767	0.6661	0.6850	0.6069	0.5648
	Logistic	0.9575	0.9486	0.9482	0.8752	0.8211	0.8582	0.7562	0.7225
	Stable	0.9771	0.9730	0.9712	0.9575	0.9876	0.9942	0.9731	0.9824
	t-Location Scale	0.9852	0.9830	0.9806	0.9629	0.9866	0.9952	0.9671	0.9725

The evaluation indices FICP, FINAW, and AWD were adopted to assess the interval forecasting results and to analyze the forecasting uncertainty of the four selected models [61]. Notably, the larger FICP values gave better analysis results, whereas larger FINAW and AWD values gave worse analysis results. The above three metrics and the lower and upper confines of the wind prediction values [62] are defined in Table 9, and the results of the uncertainty analysis are presented in Table 10. Furthermore, the expectation probability, defined as $(1 - \alpha) \times 100\%$, was set at 95%, 90%, and 85% to assess the forecasting uncertainty of the four selected models in the uncertainty analysis.

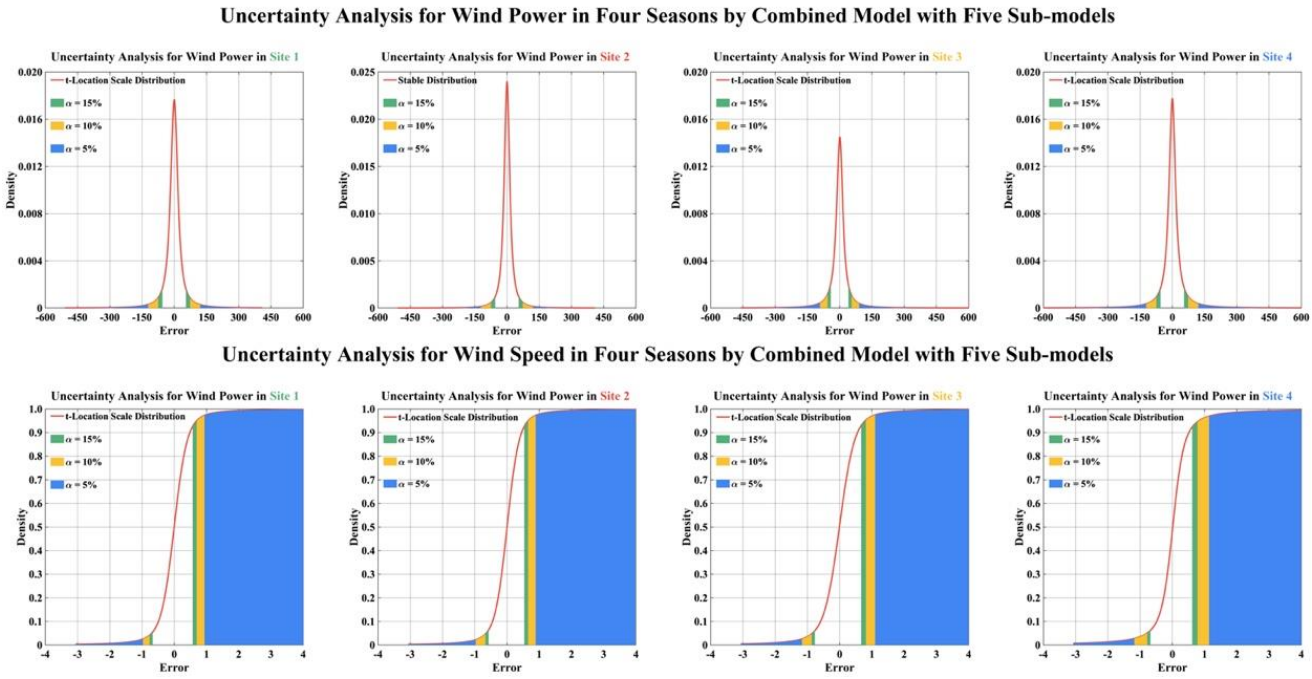

Figure 6. The optimal distribution of forecasting error in CM5.

Table 10. Evaluation Index Regulations for Uncertainty Forecasting Performance Comparison.

Metric	Definition	Equation
Upper Bound	Upper bounds of the wind speed forecasting value	$U(i) = F(i) + \frac{K_{1-0.5*\alpha} \times \sigma}{\sqrt{N}}$
Lower Bound	Lower bounds of the wind speed forecasting value	$L(i) = F(i) - \frac{K_{1-0.5*\alpha} \times \sigma}{\sqrt{N}}$
FICP	Forecast interval coverage probability of testing dataset	$\mathbf{FICP} = \frac{1}{N}\sum_{i=1}^{N} c_i \times 100\%$
FINAW	Forecast interval normalized average width of testing dataset	$\mathbf{FINAW} = \frac{1}{NR}\sum_{i=1}^{N} (U_i - L_i)$
AWD_i	Accumulated width deviation of testing sample i	$\mathbf{AMD}_i = \begin{cases} (L_i - Au_i)/(U_i - L_i), & Au_i < L_i \\ 0, & Au_i \in [L_i, U_i] \\ (Au_i - U_i)/(U_i - L_i), & Au_i > U_i \end{cases}$
AWD	Accumulated width deviation of testing dataset	$\mathbf{AMD} = \frac{1}{NR}\sum_{i=1}^{N} \mathbf{AMD}_i$

Note: $F(i)$ is the corresponding point prediction value at point i. K and σ are the quantile and scale parameters of the logistic DF. N represents the forecasting length, and NR is the difference between the maximum and minimum forecasting values. If the actual value is $Au_i \in [L_i, U_i]$, $c_i = 1$; otherwise, $c_i = 0$.

Table 11 shows that the combined model based on MODA and the five sub-models obtained satisfactory uncertainty analysis assessment results, which proves that the proposed model is superior to the other combined models. Using the wind power results for Site 1 as examples at the 15% significance level, the FICP values obtained from each combined model with different numbers of sub-models (MODA-CM2, MODA-CM3, MODA-CM4 and MODA-CM5) were found to be 77.58%, 79.71%, 81.97% and 82.96%, respectively, whereas the FINAW values were 0.0852, 0.0787, 0.0726 and 0.0694, respectively. Furthermore, the proposed model resulted in reductions in AWD values of 0.1119, 0.0645, and 0.0214, respectively, compared with the combined model with five sub-models.

Table 11. Uncertainty forecasting Performance Comparison Table of the Proposed Model and Several Competitive Models from Experiment I-III.

Site	Alpha	Metric	Uncertainty Analysis for Wind Power				Uncertainty Analysis for Wind Speed			
			MODA-CM2	MODA-CM3	MODA-CM4	MODA-CM5	MODA-CM2	MODA-CM3	MODA-CM4	MODA-CM5
Site 1	5%	FICP	92.53%	93.55%	94.64%	95.06%	90.45%	92.26%	93.82%	94.59%
		FINAW	0.1896	0.175	0.1613	0.1544	0.2337	0.2188	0.201	0.1921
		AWD	0.0597	0.0482	0.038	0.0333	8.599	6.6718	4.9176	4.0492
	10%	FICP	84.40%	86.28%	88.05%	88.79%	82.71%	85.14%	87.67%	88.99%
		FINAW	0.1155	0.1067	0.0984	0.0941	0.1734	0.1625	0.1492	0.1425
		AWD	0.1849	0.1557	0.1299	0.117	20.5692	16.7262	12.9613	11.1074
	15%	FICP	77.58%	79.71%	81.97%	82.96%	76.17%	78.97%	82.02%	83.53%
		FINAW	0.0852	0.0787	0.0726	0.0694	0.142	0.1331	0.1222	0.1168
		AWD	0.3338	0.2864	0.2433	0.2219	34.0823	28.3738	22.5981	19.7348
Site 2	5%	FICP	92.68%	93.85%	94.64%	95.14%	90.72%	92.36%	94.07%	94.82%
		FINAW	0.1335	0.1228	0.1126	0.1073	0.2025	0.1871	0.1713	0.1634
		AWD	0.0735	0.0606	0.0494	0.0437	8.0195	6.1951	4.578	3.8903
	10%	FICP	84.97%	86.61%	88.19%	88.91%	83.11%	85.39%	87.50%	89.01%
		FINAW	0.0828	0.0762	0.0699	0.0666	0.1487	0.1374	0.1258	0.12
		AWD	0.2025	0.1718	0.1439	0.1296	19.2918	15.5357	12.1406	10.5021
	15%	FICP	78.08%	80.26%	82.54%	83.71%	75.92%	79.32%	82.39%	83.73%
		FINAW	0.0616	0.0568	0.052	0.0496	0.1212	0.1119	0.1025	0.0978
		AWD	0.3513	0.3021	0.2566	0.2336	32.0718	26.3358	21.115	18.5686
Site 3	5%	FICP	93.15%	94.05%	95.14%	95.68%	90.20%	92.24%	93.70%	94.44%
		FINAW	0.2619	0.2455	0.2277	0.2189	0.2385	0.2191	0.1995	0.1903
		AWD	0.0491	0.0399	0.0312	0.027	7.3483	5.4847	3.9785	3.3008
	10%	FICP	84.13%	86.19%	87.95%	88.59%	83.04%	85.32%	87.75%	88.74%
		FINAW	0.1525	0.1429	0.1327	0.1276	0.1767	0.1624	0.1481	0.1411
		AWD	0.1741	0.1488	0.1237	0.1118	17.7187	14.0368	10.8555	9.3221
	15%	FICP	76.74%	78.77%	80.51%	81.65%	76.26%	79.19%	82.07%	83.73%
		FINAW	0.1098	0.1029	0.0956	0.0919	0.1447	0.1329	0.1213	0.1156
		AWD	0.3334	0.2907	0.2474	0.2262	29.4085	23.8798	18.9585	16.5917
Site 4	5%	FICP	93.63%	94.44%	95.31%	95.76%	91.52%	93.15%	94.47%	95.16%
		FINAW	0.2422	0.2245	0.2099	0.2023	0.2375	0.2214	0.2048	0.1956
		AWD	0.0426	0.0342	0.0267	0.0233	6.8928	5.3731	4.0268	3.3892
	10%	FICP	84.80%	85.94%	87.57%	88.42%	82.66%	84.67%	87.10%	88.19%
		FINAW	0.1337	0.1238	0.1158	0.1117	0.1621	0.1512	0.1398	0.1336
		AWD	0.1691	0.1438	0.1208	0.1098	19.9071	16.2968	12.9652	11.3022
	15%	FICP	77.18%	79.37%	81.45%	82.49%	76.22%	78.70%	81.00%	82.24%
		FINAW	0.0935	0.0866	0.081	0.0781	0.1271	0.1185	0.1096	0.1047
		AWD	0.3311	0.2873	0.2487	0.2298	34.924	29.4457	24.1466	21.4982

5. Conclusions

As an important source of clean energy, the use of wind energy has undergone rapid development, becoming widespread in recent years. However, the irregularity and instability of wind speed series data greatly restricts the development of wind power generation. There is an urgent need to successfully and accurately forecast wind speed and wind power, solve the dispatch problem, and further improve the operation efficiency of the power market. In this study, a combined model for wind speed and wind power day-ahead forecasting was developed. First, the original wind speed and wind energy time series were preprocessed using the secondary denoising method. Then, nine different ANN and machine learning forecasting models were established to forecast the wind speed and wind energy time series after denoising.

By assessing the accuracy of the model validation set, the optimal sub-model was selected for the combined model. Finally, the combined weight of the combined model was optimized by the multi-objective optimization algorithm. Considering the wind speed forecasting results, the MAPE of the optimal combined model was between 5.86% and 11.92%, the R^2 was over 0.94, and the RMSE was between 0.3379 and 0.7595. Furthermore, the corresponding values for wind power forecasting were in the range of 11.10% to 33.05%, over 0.97, and between 0.10102 and 0.33641, respectively. All of the experimental results indicate that the combined forecasting system has high levels of accuracy and stability for wind speed and wind power forecasting.

Author Contributions: The experiment, data analysis, and paper writing were conducted by Q.L.; the experiment and data analysis were completed by Q.L. and Q.Z.; supervision, paper writing, and editing were conducted by Q.Z. and G.Z.; validation, methodology, paper editing, and supervision were handled by Q.L. and G.Z. All authors have read and agreed to the published version of the manuscript.

Funding: This research was funded by State Grid Corporation of China Science and Technology Project: SGGSKY00WYJS2000062.

Conflicts of Interest: The authors declare no conflict of interest.

Appendix A

Modified Multi-Objective Dragonfly Algorithm

In order to solve the problems associated with the MODA of easily falling into local optimal solutions and having slower convergence speeds, a steps-based strategy based on an exponential function and an elite opposition learning strategy were used for modification. First, the elite opposition learning strategy was used to generate a broader search scope and diversify the population identified as the next generation and to improve the global search capacity and search accuracy of the MODA [62]. Then, a steps-based strategy based on an exponential function was applied to enhance the convergence speed of the algorithm in the later stages. The specific implementation scheme is as follows:

(1) Elite Opposition Learning Strategy

To improve the global search capacity and search accuracy of the MODA, the elite opposition learning strategy was applied to produce various elite opposition individuals and further develop an unplanned opposition population that can hunt in neighborhood space and enhance the local mining capacity. During the running of the MODA, the elite opposition learning strategy can define the elite dragonfly as the top dragonfly with the best fitness value. This is expressed by $\mathbf{ex}_m^t = [ex_{m,1}^t, ex_{m,2}^t, \cdots, ex_{m,D}^t]$, $m = 1, 2, \ldots, EN$, where $ex_{i,j}^t$ indicates the elite solutions corresponding to individuals $x_{i,j}^t$, t is the present iteration, and D represents the dimension of the algorithm space.

Moreover, an elite opposition solution $\tilde{\mathbf{ex}}_i^t = [\breve{ex}_{i,1}^t, \breve{ex}_{i,2}^t, \cdots, \breve{ex}_{i,D}^t]$ with respect to a certain dragonfly in the current solution $\mathbf{x}_i^t = [x_{i,1}^t, x_{i,2}^t, \cdots, x_{i,D}^t]$ can be mathematically modeled by:

$$\breve{ex}_{i,j}^t = k \cdot (\mathbf{ea}_j^t + \mathbf{eb}_j^t) - x_{i,j}^t. \tag{A1}$$

$$\mathbf{ea}_j^t = min(ex_{m,j}^t), \mathbf{eb}_j^t = max(ex_{m,j}^t). \tag{A2}$$

$$\breve{ex}_{i,j}^t = rand \cdot (\mathbf{eb}_j^t - \mathbf{ea}_j^t) + \mathbf{ea}_j^t, \text{ if } \breve{ex}_{i,j}^t < L\mathbf{b}_i. \tag{A3}$$

where $i = 1, 2, \ldots, SN$, $j = 1, 2, \ldots, EN$, $k = rand(0, 1)$, SN represents the population size of the dragonflies, and, generally, EN represents the selected number of elite individuals with the value of SN*0.1. k represents a generalized argument that is subject to a uniform distribution. The elite opposition learning strategy is used in the basic MODA to effectively expand the search area, diversify the population, and enhance the optimization performance and global search capability.

(2) Steps-based Strategy based on an Exponential Function

In a basic MODA, there are several parameters ($s, a, c, f, e,$ and w), as described by $\Delta\mathbf{x}_{t+1} = (sS_i + aA_i + cC_i + fF_i + eE_i) + w\mathbf{x}_t$, which are adaptively adjusted at random; hence, the dragonfly individuals update themselves according to a stochastic linear step size in the course of iteration. This means that the position update of the dragonfly completely relies on the site of the present individual and the stochastic linear step size, which can be determined, respectively. Despite the above strategy being conducive to finding a globally optimal solution to some degree, it cannot ensure that the solution is optimal; thus, this situation causes a slow convergence rate [51]. To expedite the convergence rate of the

MODA, the exponential step strategy is applied to replace the original linear step strategy. This means that an exponential function is added to the original step and generates an exponential function steps-based strategy. It should be noted that a vital parameter μ is adopted to renew the step, so that the local and global hunt capacities can be improved, and the convergence rate can be further accelerated. Hence, it is pivotal to set a suitable μ.

In our study, the steps were updated based on the following exponential function:

$$\mu = (rand - 0.5) \cdot 2^{rand} \tag{A4}$$

The enhanced step-size rule used is:

$$\Delta = \mu \cdot \Delta \mathbf{x}_{t+1} = (rand - 0.5) \cdot 2^{rand} \cdot \Delta \mathbf{x}_{t+1} \tag{A5}$$

Here, $rand \in [0, 1]$ is a stochastic constant, and $\Delta \mathbf{x}_t$ is the step size in the tth iteration. The equation for updating the position vector of dragonflies is expressed by:

$$\mathbf{x}_{t+1} = \mathbf{x}_t + \mu \cdot \Delta \mathbf{x}_t + 1 = \mathbf{x}_t + (rand - 0.5) \cdot 2^{rand} \cdot \Delta \mathbf{x}_{t+1} \tag{A6}$$

In the above, t is the current iteration, and $\mathbf{x}_t$ is the position vector in the tth iteration.

Apparently, the updating speed of the step size accelerates as the number of iterations increases. At the beginning of an iteration, the advanced step can accomplish local hunting and discover a more optimal hunt space. During the medium and later periods in the course of iteration, the advanced step will accelerate the convergence rate, avoiding the local optimum and finding the optimal solution in the global hunt process.

Table A1. The forecasting performance of five optimal sub-models for wind speed and wind power in the first season.

Site	Metric	Wind Speed Forecasting Results					Wind Power Forecasting Results				
		LSTM	**WNN**	**ANFIS**	**RNN**	**ELM**	**LSTM**	**Elman**	**BPNN**	**RBFNN**	**SVM**
Site 1	MAE	0.7128	0.8047	0.9306	0.9952	1.1224	72.7578	84.7192	94.2429	100.1841	123.008
	RMSE	0.9969	1.0498	1.213	1.316	1.4909	123.6352	138.1371	150.2004	159.6466	191.7045
	STDAPE	14.22%	15.16%	17.65%	18.85%	20.90%	80.87%	136.27%	153.49%	172.28%	260.26%
	DA	53.23%	47.27%	44.39%	47.47%	44.59%	50.05%	44.49%	45.08%	43.40%	40.81%
	U1	0.0902	0.0951	0.1093	0.1182	0.1329	0.1144	0.1281	0.1389	0.1467	0.1749
	U2	0.8881	0.871	1.0413	1.085	1.4672	0.4916	0.5218	0.5837	0.6357	1.7005
	MAPE	14.91%	17.05%	20.06%	21.49%	24.03%	28.53%	35.87%	37.62%	43.22%	55.27%
	R^2	0.896	0.8831	0.8451	0.8182	0.7771	0.9411	0.9257	0.9121	0.9022	0.8603
Site	**Metric**	**LSTM**	**WNN**	**ELM**	**RNN**	**ANFIS**	**LSTM**	**Elman**	**BPNN**	**SVM**	**RBFNN**
Site 2	MAE	0.6592	0.7582	0.8299	0.9609	1.113	55.2501	64.6423	68.5449	81.2518	92.9089
	RMSE	0.9157	1.0199	1.1101	1.2878	1.4649	94.3334	101.4713	107.9959	129.0841	146.0998
	STDAPE	15.65%	18.03%	18.53%	20.95%	26.19%	105.16%	234.08%	255.50%	348.94%	427.78%
	DA	52.33%	46.57%	47.57%	43.00%	42.60%	50.35%	42.30%	44.69%	41.31%	39.82%
	U1	0.0926	0.1028	0.1118	0.1291	0.1459	0.1092	0.1169	0.1233	0.1476	0.1652
	U2	1.0602	1.1315	1.2836	1.5189	1.8958	0.827	0.7993	0.7507	0.7423	0.6758
	MAPE	15.81%	18.63%	20.35%	23.44%	27.72%	31.61%	45.31%	52.43%	62.54%	75.86%
	R^2	0.9078	0.8857	0.8658	0.8221	0.7738	0.9575	0.9499	0.9432	0.918	0.8969
Site	**Metric**	**LSTM**	**RNN**	**ELM**	**WNN**	**ANFIS**	**Elman**	**LSTM**	**BPNN**	**RBFNN**	**ANFIS**
Site 3	MAE	0.7401	0.8572	0.9891	1.1429	1.2817	86.0772	102.83	110.7717	124.926	141.6915
	RMSE	1.0265	1.1234	1.2926	1.4726	1.6495	143.5346	167.6258	174.9203	191.9277	213.2843
	STDAPE	16.57%	17.86%	22.35%	23.63%	27.92%	184.14%	241.75%	270.58%	331.04%	381.07%
	DA	52.04%	46.38%	43.50%	40.32%	42.01%	52.14%	44.89%	44.79%	45.38%	41.81%
	U1	0.0921	0.1009	0.1155	0.1309	0.1453	0.1367	0.1592	0.165	0.1777	0.1965
	U2	0.9028	1.0113	1.1226	1.2138	1.43	0.7837	0.8137	0.7846	0.7471	0.7233
	MAPE	16.43%	18.98%	22.27%	25.56%	29.17%	38.51%	48.10%	55.41%	64.25%	75.54%
	R^2	0.8932	0.872	0.8308	0.7842	0.745	0.9216	0.893	0.8834	0.8661	0.8373
Site	**Metric**	**ANFIS**	**WNN**	**ELM**	**RNN**	**NARNN**	**ANFIS**	**BPNN**	**RBFNN**	**Elman**	**GRNN**
Site 4	MAE	0.783	0.8931	1.0345	1.18	1.3166	90.0454	107.0139	117.4349	132.8439	154.0333
	RMSE	1.1462	1.2293	1.4323	1.6254	1.803	152.6258	173.0959	180.8868	213.9421	228.7902
	STDAPE	18.73%	21.71%	25.73%	27.44%	28.79%	64.24%	79.57%	123.60%	153.34%	149.54%
	DA	51.14%	48.36%	43.89%	42.40%	39.52%	48.56%	44.19%	46.08%	43.59%	41.51%
	U1	0.0914	0.098	0.1136	0.1286	0.1422	0.1235	0.14	0.1451	0.1679	0.1794
	U2	1.1756	1.0218	1.2242	1.4279	1.5687	0.9525	0.9708	0.998	0.6264	0.7754
	MAPE	15.00%	17.86%	20.74%	23.37%	25.91%	29.34%	36.77%	45.06%	53.03%	61.99%
	R^2	0.8821	0.8631	0.8156	0.7734	0.7272	0.9227	0.8995	0.8909	0.8598	0.8351

Table A2. The forecasting performance of five optimal sub-models for wind speed and wind power in the second season.

Site	Metric	Wind Speed Forecasting Results					Wind Power Forecasting Results				
		LSTM	**WNN**	**RNN**	**ANFIS**	**ELM**	**LSTM**	**Elman**	**BPNN**	**RBFNN**	**SVM**
Site 1	MAE	0.7128	0.8047	0.9306	0.9952	1.1224	72.7578	84.7192	94.2429	100.1841	123.008
	RMSE	0.9969	1.0498	1.213	1.316	1.4909	123.6352	138.1371	150.2004	159.6466	191.7045
	STDAPE	14.22%	15.16%	17.65%	18.85%	20.90%	80.87%	136.27%	153.49%	172.28%	260.26%
	DA	53.23%	47.27%	44.39%	47.47%	44.59%	50.05%	44.49%	45.08%	43.40%	40.81%
	U1	0.0902	0.0951	0.1093	0.1182	0.1329	0.1144	0.1281	0.1389	0.1467	0.1749
	U2	0.8881	0.871	1.0413	1.085	1.4672	0.4916	0.5218	0.5837	0.6357	1.7005
	MAPE	14.91%	17.05%	20.06%	21.49%	24.03%	28.53%	35.87%	37.62%	43.22%	55.27%
	R^2	0.896	0.8831	0.8451	0.8182	0.7771	0.9411	0.9257	0.9121	0.9022	0.8603
Site	**Metric**	**LSTM**	**ELM**	**RNN**	**WNN**	**ANFIS**	**LSTM**	**Elman**	**BPNN**	**SVM**	**RBFNN**
Site 2	MAE	0.6592	0.7582	0.8299	0.9609	1.113	55.2501	64.6423	68.5449	81.2518	92.9089
	RMSE	0.9157	1.0199	1.1101	1.2878	1.4649	94.3334	101.4713	107.9959	129.0841	146.0998
	STDAPE	15.65%	18.03%	18.53%	20.95%	26.19%	105.16%	234.08%	255.50%	348.94%	427.78%
	DA	52.33%	46.57%	47.57%	43.00%	42.60%	50.35%	42.30%	44.69%	41.31%	39.82%
	U1	0.0926	0.1028	0.1118	0.1291	0.1459	0.1092	0.1169	0.1233	0.1476	0.1652
	U2	1.0602	1.1315	1.2836	1.5189	1.8958	0.827	0.7993	0.7507	0.7423	0.6758
	MAPE	15.81%	18.63%	20.35%	23.44%	27.72%	31.61%	45.31%	52.43%	62.54%	75.86%
	R^2	0.9078	0.8857	0.8658	0.8221	0.7738	0.9575	0.9499	0.9432	0.918	0.8969
Site	**Metric**	**LSTM**	**WNN**	**ELM**	**RNN**	**ANFIS**	**LSTM**	**Elman**	**BPNN**	**ANFIS**	**SVM**
Site 3	MAE	0.7401	0.8572	0.9891	1.1429	1.2817	86.0772	102.83	110.7717	124.926	141.6915
	RMSE	1.0265	1.1234	1.2926	1.4726	1.6495	143.5346	167.6258	174.9203	191.9277	213.2843
	STDAPE	16.57%	17.86%	22.35%	23.63%	27.92%	184.14%	241.75%	270.58%	331.04%	381.07%
	DA	52.04%	46.38%	43.50%	40.32%	42.01%	52.14%	44.89%	44.79%	45.38%	41.81%
	U1	0.0921	0.1009	0.1155	0.1309	0.1453	0.1367	0.1592	0.165	0.1777	0.1965
	U2	0.9028	1.0113	1.1226	1.2138	1.43	0.7837	0.8137	0.7846	0.7471	0.7233
	MAPE	16.43%	18.98%	22.27%	25.56%	29.17%	38.51%	48.10%	55.41%	64.25%	75.54%
	R^2	0.8932	0.872	0.8308	0.7842	0.745	0.9216	0.893	0.8834	0.8661	0.8373
Site	**Metric**	**ANFIS**	**WNN**	**ELM**	**RNN**	**NARNN**	**BPNN**	**Elman**	**LSTM**	**ANFIS**	**RBFNN**
Site 4	MAE	0.783	0.8931	1.0345	1.18	1.3166	90.0454	107.0139	117.4349	132.8439	154.0333
	RMSE	1.1462	1.2293	1.4323	1.6254	1.803	152.6258	173.0959	180.8868	213.9421	228.7902
	STDAPE	18.73%	21.71%	25.73%	27.44%	28.79%	64.24%	79.57%	123.60%	153.34%	149.54%
	DA	51.14%	48.36%	43.89%	42.40%	39.52%	48.56%	44.19%	46.08%	43.59%	41.51%
	U1	0.0914	0.098	0.1136	0.1286	0.1422	0.1235	0.14	0.1451	0.1679	0.1794
	U2	1.1756	1.0218	1.2242	1.4279	1.5687	0.9525	0.9708	0.998	0.6264	0.7754
	MAPE	15.00%	17.86%	20.74%	23.37%	25.91%	29.34%	36.77%	45.06%	53.03%	61.99%
	R^2	0.8821	0.8631	0.8156	0.7734	0.7272	0.9227	0.8995	0.8909	0.8598	0.8351

Table A3. The forecasting performance of five optimal sub-models for wind speed and wind power in the third season.

Site	Metric	Wind Speed Forecasting Results					Wind Power Forecasting Results				
		LSTM	**WNN**	**ANFIS**	**RNN**	**ELM**	**LSTM**	**Elman**	**BPNN**	**RBFNN**	**SVM**
Site 1	MAE	0.7128	0.8047	0.9306	0.9952	1.1224	72.7578	84.7192	94.2429	100.1841	123.008
	RMSE	0.9969	1.0498	1.213	1.316	1.4909	123.6352	138.1371	150.2004	159.6466	191.7045
	STDAPE	14.22%	15.16%	17.65%	18.85%	20.90%	80.87%	136.27%	153.49%	172.28%	260.26%
	DA	53.23%	47.27%	44.39%	47.47%	44.59%	50.05%	44.49%	45.08%	43.40%	40.81%
	U1	0.0902	0.0951	0.1093	0.1182	0.1329	0.1144	0.1281	0.1389	0.1467	0.1749
	U2	0.8881	0.871	1.0413	1.085	1.4672	0.4916	0.5218	0.5837	0.6357	1.7005
	MAPE	14.91%	17.05%	20.06%	21.49%	24.03%	28.53%	35.87%	37.62%	43.22%	55.27%
	R^2	0.896	0.8831	0.8451	0.8182	0.7771	0.9411	0.9257	0.9121	0.9022	0.8603
Site	**Metric**	**LSTM**	**ELM**	**RNN**	**WNN**	**ANFIS**	**LSTM**	**Elman**	**BPNN**	**RBFNN**	**SVM**
Site 2	MAE	0.6592	0.7582	0.8299	0.9609	1.113	55.2501	64.6423	68.5449	81.2518	92.9089
	RMSE	0.9157	1.0199	1.1101	1.2878	1.4649	94.3334	101.4713	107.9959	129.0841	146.0998
	STDAPE	15.65%	18.03%	18.53%	20.95%	26.19%	105.16%	234.08%	255.50%	348.94%	427.78%
	DA	52.33%	46.57%	47.57%	43.00%	42.60%	50.35%	42.30%	44.69%	41.31%	39.82%
	U1	0.0926	0.1028	0.1118	0.1291	0.1459	0.1092	0.1169	0.1233	0.1476	0.1652
	U2	1.0602	1.1315	1.2836	1.5189	1.8958	0.827	0.7993	0.7507	0.7423	0.6758
	MAPE	15.81%	18.63%	20.35%	23.44%	27.72%	31.61%	45.31%	52.43%	62.54%	75.86%
	R^2	0.9078	0.8857	0.8658	0.8221	0.7738	0.9575	0.9499	0.9432	0.918	0.8969
Site	**Metric**	**LSTM**	**RNN**	**WNN**	**ELM**	**ANFIS**	**LSTM**	**Elman**	**BPNN**	**RBFNN**	**SVM**
Site 3	MAE	0.7401	0.8572	0.9891	1.1429	1.2817	86.0772	102.83	110.7717	124.926	141.6915
	RMSE	1.0265	1.1234	1.2926	1.4726	1.6495	143.5346	167.6258	174.9203	191.9277	213.2843
	STDAPE	16.57%	17.86%	22.35%	23.63%	27.92%	184.14%	241.75%	270.58%	331.04%	381.07%
	DA	52.04%	46.38%	43.50%	40.32%	42.01%	52.14%	44.89%	44.79%	45.38%	41.81%
	U1	0.0921	0.1009	0.1155	0.1309	0.1453	0.1367	0.1592	0.165	0.1777	0.1965
	U2	0.9028	1.0113	1.1226	1.2138	1.43	0.7837	0.8137	0.7846	0.7471	0.7233
	MAPE	16.43%	18.98%	22.27%	25.56%	29.17%	38.51%	48.10%	55.41%	64.25%	75.54%
	R^2	0.8932	0.872	0.8308	0.7842	0.745	0.9216	0.893	0.8834	0.8661	0.8373

Table A3. *Cont.*

Site	Metric	Wind Speed Forecasting Results					Wind Power Forecasting Results				
		LSTM	**WNN**	**ANFIS**	**RNN**	**ELM**	**LSTM**	**Elman**	**BPNN**	**RBFNN**	**SVM**
Site	**Metric**	**ANFIS**	**RNN**	**WNN**	**ELM**	**NARNN**	**BPNN**	**ANFIS**	**Elman**	**RBFNN**	**GRNN**
Site 4	MAE	0.783	0.8931	1.0345	1.18	1.3166	90.0454	107.0139	117.4349	132.8439	154.0333
	RMSE	1.1462	1.2293	1.4323	1.6254	1.803	152.6258	173.0959	180.8868	213.9421	228.7902
	STDAPE	18.73%	21.71%	25.73%	27.44%	28.79%	64.24%	79.57%	123.60%	153.34%	149.54%
	DA	51.14%	48.36%	43.89%	42.40%	39.52%	48.56%	44.19%	46.08%	43.59%	41.51%
	U1	0.0914	0.098	0.1136	0.1286	0.1422	0.1235	0.14	0.1451	0.1679	0.1794
	U2	1.1756	1.0218	1.2242	1.4279	1.5687	0.9525	0.9708	0.998	0.6264	0.7754
	MAPE	15.00%	17.86%	20.74%	23.37%	25.91%	29.34%	36.77%	45.06%	53.03%	61.99%
	R^2	0.8821	0.8631	0.8156	0.7734	0.7272	0.9227	0.8995	0.8909	0.8598	0.8351

Table A4. The forecasting performance of five optimal sub-models for wind speed and wind power in the fourth season.

Site	Metric	Wind Speed Forecasting Results					Wind Power Forecasting Results				
		LSTM	**ANFIS**	**RNN**	**ELM**	**WNN**	**LSTM**	**Elman**	**BPNN**	**RBFNN**	**SVM**
Site 1	MAE	0.7128	0.8047	0.9306	0.9952	1.1224	72.7578	84.7192	94.2429	100.1841	123.008
	RMSE	0.9969	1.0498	1.213	1.316	1.4909	123.6352	138.1371	150.2004	159.6466	191.7045
	STDAPE	14.22%	15.16%	17.65%	18.85%	20.90%	80.87%	136.27%	153.49%	172.28%	260.26%
	DA	53.23%	47.27%	44.39%	47.47%	44.59%	50.05%	44.49%	45.08%	43.40%	40.81%
	U1	0.0902	0.0951	0.1093	0.1182	0.1329	0.1144	0.1281	0.1389	0.1467	0.1749
	U2	0.8881	0.871	1.0413	1.085	1.4672	0.4916	0.5218	0.5837	0.6357	1.7005
	MAPE	14.91%	17.05%	20.06%	21.49%	24.03%	28.53%	35.87%	37.62%	43.22%	55.27%
	R^2	0.896	0.8831	0.8451	0.8182	0.7771	0.9411	0.9257	0.9121	0.9022	0.8603
Site	**Metric**	**LSTM**	**RNN**	**WNN**	**ELM**	**ANFIS**	**LSTM**	**Elman**	**BPNN**	**SVM**	**RBFNN**
Site 2	MAE	0.6592	0.7582	0.8299	0.9609	1.113	55.2501	64.6423	68.5449	81.2518	92.9089
	RMSE	0.9157	1.0199	1.1101	1.2878	1.4649	94.3334	101.4713	107.9959	129.0841	146.0998
	STDAPE	15.65%	18.03%	18.53%	20.95%	26.19%	105.16%	234.08%	255.50%	348.94%	427.78%
	DA	52.33%	46.57%	47.57%	43.00%	42.60%	50.35%	42.30%	44.69%	41.31%	39.82%
	U1	0.0926	0.1028	0.1118	0.1291	0.1459	0.1092	0.1169	0.1233	0.1476	0.1652
	U2	1.0602	1.1315	1.2836	1.5189	1.8958	0.827	0.7993	0.7507	0.7423	0.6758
	MAPE	15.81%	18.63%	20.35%	23.44%	27.72%	31.61%	45.31%	52.43%	62.54%	75.86%
	R^2	0.9078	0.8857	0.8658	0.8221	0.7738	0.9575	0.9499	0.9432	0.918	0.8969
Site	**Metric**	**LSTM**	**WNN**	**RNN**	**ELM**	**ANFIS**	**Elman**	**LSTM**	**BPNN**	**SVM**	**RBFNN**
Site 3	MAE	0.7401	0.8572	0.9891	1.1429	1.2817	86.0772	102.83	110.7717	124.926	141.6915
	RMSE	1.0265	1.1234	1.2926	1.4726	1.6495	143.5346	167.6258	174.9203	191.9277	213.2843
	STDAPE	16.57%	17.86%	22.35%	23.63%	27.92%	184.14%	241.75%	270.58%	331.04%	381.07%
	DA	52.04%	46.38%	43.50%	40.32%	42.01%	52.14%	44.89%	44.79%	45.38%	41.81%
	U1	0.0921	0.1009	0.1155	0.1309	0.1453	0.1367	0.1592	0.165	0.1777	0.1965
	U2	0.9028	1.0113	1.1226	1.2138	1.43	0.7837	0.8137	0.7846	0.7471	0.7233
	MAPE	16.43%	18.98%	22.27%	25.56%	29.17%	38.51%	48.10%	55.41%	64.25%	75.54%
	R^2	0.8932	0.872	0.8308	0.7842	0.745	0.9216	0.893	0.8834	0.8661	0.8373
Site	**Metric**	**ANFIS**	**WNN**	**ELM**	**RNN**	**NARNN**	**Elman**	**BPNN**	**RBFNN**	**ANFIS**	**GRNN**
Site 4	MAE	0.783	0.8931	1.0345	1.18	1.3166	90.0454	107.0139	117.4349	132.8439	154.0333
	RMSE	1.1462	1.2293	1.4323	1.6254	1.803	152.6258	173.0959	180.8868	213.9421	228.7902
	STDAPE	18.73%	21.71%	25.73%	27.44%	28.79%	64.24%	79.57%	123.60%	153.34%	149.54%
	DA	51.14%	48.36%	43.89%	42.40%	39.52%	48.56%	44.19%	46.08%	43.59%	41.51%
	U1	0.0914	0.098	0.1136	0.1286	0.1422	0.1235	0.14	0.1451	0.1679	0.1794
	U2	1.1756	1.0218	1.2242	1.4279	1.5687	0.9525	0.9708	0.998	0.6264	0.7754
	MAPE	15.00%	17.86%	20.74%	23.37%	25.91%	29.34%	36.77%	45.06%	53.03%	61.99%
	R^2	0.8821	0.8631	0.8156	0.7734	0.7272	0.9227	0.8995	0.8909	0.8598	0.8351

Table A5. The test result of two types of time series by each sub-model.

Type	Period	1st Season											
	Site	Site 1			Site 2			Site 3			Site 4		
	Model	DM Test	WRS Test	Model	DM Test	WRS Test	Model	DM Test	WRS Test	Model	DM Test	WRS Test
Wind Speed	LSTM	2.0153 *	0.3999 (1)	LSTM	2.2311 *	0.5271 (1)	LSTM	2.1936 *	0.5866 (1)	ANFIS	2.0345 *	0.7851 (1)
	WNN	2.0911 *	0.5008 (1)	WNN	2.3116 *	0.4679 (1)	RNN	2.3051 *	0.4623 (1)	WNN	2.0683 *	0.8657 (1)
	ANFIS	2.0791 *	0.6388 (1)	ELM	2.2490 *	0.4506 (1)	ELM	2.2691 *	0.9545 (1)	ELM	2.0176 *	0.8652 (1)
	RNN	2.0237 *	0.8169 (1)	RNN	2.2329 *	0.5504 (1)	WNN	2.2762 *	0.7556 (1)	RNN	2.0892 *	0.8939 (1)
	ELM	2.0347 *	0.9344 (1)	ANFIS	2.2511 *	0.9087 (1)	ANFIS	2.2555 *	0.4812 (1)	NARNN	2.0554 *	0.9906 (1)
Wind Power	LSTM	1.6448 **	0.5148 (1)	LSTM	1.8413 **	0.1658 (1)	Elman	2.1714 *	0.469 (1)	ANFIS	1.8767 **	0.5515 (1)
	Elman	1.8584 **	0.6926 (1)	Elman	2.0113 *	0.3029 (1)	LSTM	2.1891 *	0.428 (1)	BPNN	1.8933 **	0.7224 (1)
	BPNN	1.8545 **	0.7135 (1)	BPNN	1.9819 *	0.3315 (1)	BPNN	2.1510 *	0.8385 (1)	RBFNN	1.9811 *	0.9577 (1)
	RBFNN	1.8092 **	0.6182 (1)	SVM	1.9397 **	0.4709 (1)	RBFNN	2.1536 *	0.883 (1)	Elman	1.8210 **	0.8973 (1)
	SVM	1.6948 **	0.9221 (1)	RBFNN	1.9759 *	0.6006 (1)	ANFIS	2.1529 *	0.8701 (1)	GRNN	1.9347 **	0.6005 (1)
Type	**Period**	**2nd Season**											
Wind Speed	LSTM	2.1945 *	0.6758 (1)	LSTM	2.2025 *	0.4777 (1)	LSTM	2.1799 *	0.5881 (1)	ANFIS	2.1549 *	0.9343 (1)
	WNN	2.0491 *	0.7707 (1)	ELM	2.1907 *	0.3819 (1)	WNN	2.1802 *	0.6535 (1)	WNN	2.1582 *	0.8213 (1)
	RNN	2.1712 *	0.9856 (1)	RNN	2.1570 *	0.4754 (1)	ELM	2.1139 *	0.7227 (1)	ELM	2.1066 *	0.4826 (1)
	ANFIS	2.2617 *	0.9507 (1)	WNN	2.1710 *	0.6418 (1)	RNN	2.1974 *	0.8559 (1)	RNN	2.1212 *	0.3952 (1)
	ELM	2.2046 *	0.7191 (1)	ANFIS	2.1974 *	0.6615 (1)	ANFIS	2.2154 *	0.8648 (1)	NARNN	2.1212 *	0.5641 (1)
Wind Power	LSTM	1.8129 **	0.6877 (1)	LSTM	1.9293 *	0.2834 (1)	LSTM	1.8850 **	0.191 (1)	BPNN	1.9729 *	0.8058 (1)
	Elman	1.7532 **	0.5882 (1)	Elman	1.8266 **	0.5608 (1)	Elman	1.7569 **	0.652 (1)	Elman	1.9529 **	0.7731 (1)
	BPNN	1.7520 **	0.6515 (1)	BPNN	1.7419 **	0.8147 (1)	BPNN	1.7442 **	0.6615 (1)	LSTM	1.9488 **	0.8387 (1)
	RBFNN	1.7478 **	0.8189 (1)	SVM	1.9149 **	0.9142 (1)	ANFIS	1.7942 **	0.8653 (1)	ANFIS	1.9671 *	0.796 (1)
	SVM	1.7491 **	0.8162 (1)	RBFNN	1.7790 *	0.9952 (1)	SVM	1.8647 **	0.8221 (1)	RBFNN	1.9611 *	0.7553 (1)
Type	**Period**	**3rd Season**											
Wind Speed	LSTM	2.1481 *	0.3747 (1)	LSTM	2.1868 *	0.403 (1)	LSTM	2.2618 *	0.3518 (1)	ANFIS	2.0569 *	0.5237 (1)
	WNN	2.2647 *	0.6465 (1)	ELM	2.1580 *	0.4889 (1)	RNN	2.2334 *	0.5056 (1)	RNN	2.0278 *	0.814 (1)
	ANFIS	2.2909 *	0.7413 (1)	RNN	2.0821 *	0.5868 (1)	WNN	2.2084 *	0.9067 (1)	WNN	2.0900 *	0.6827 (1)
	RNN	2.2743 *	0.7856 (1)	WNN	2.1309 *	0.979 (1)	ELM	2.1865 *	0.3958 (1)	ELM	2.0578 *	0.8486 (1)
	ELM	2.2512 *	0.6406 (1)	ANFIS	2.1179 *	0.8809 (1)	ANFIS	2.1745 *	0.9007 (1)	NARNN	2.0572 *	0.7602 (1)
Wind Power	LSTM	1.8928 **	0.4611 (1)	LSTM	1.6638 **	0.3403 (1)	LSTM	2.0381 *	0.0666 (1)	BPNN	1.7334 **	0.2531 (1)
	Elman	1.8541 **	0.5106 (1)	Elman	1.6214 ***	0.185 (1)	Elman	2.1068 *	0.1145 (1)	ANFIS	1.8031 **	0.5048 (1)
	BPNN	1.8038 **	0.4511 (1)	BPNN	1.7245 **	0.7108 (1)	BPNN	2.0731 *	0.5217 (1)	Elman	1.8146 **	0.9873 (1)
	RBFNN	1.9330 **	0.8213 (1)	RBFNN	1.6877 **	0.7228 (1)	RBFNN	2.0916 *	0.9811 (1)	RBFNN	1.9499 **	0.7887 (1)
	SVM	1.8470 **	0.7011 (1)	SVM	1.7908 **	0.8306 (1)	SVM	2.1666 *	0.6872 (1)	GRNN	1.8161 **	0.9878 (1)
Type	**Period**	**4th Season**											
Wind Speed	LSTM	2.2046 *	0.8297 (1)	LSTM	2.1795 *	0.5349 (1)	LSTM	2.1252 *	0.3748 (1)	ANFIS	2.1443 *	0.2156 (1)
	ANFIS	2.2263 *	0.9765 (1)	RNN	2.1626 *	0.6195 (1)	WNN	2.1970 *	0.4513 (1)	WNN	2.1105 *	0.2088 (1)
	RNN	2.2232 *	0.9149 (1)	WNN	2.1002 *	0.8759 (1)	RNN	2.1791 *	0.9334 (1)	ELM	2.0785 *	0.6151 (1)
	ELM	2.1759 *	0.953 (1)	ELM	2.1286 *	0.9552 (1)	ELM	2.1603 *	0.7556 (1)	RNN	2.1600 *	0.8181 (1)
	WNN	2.2367 *	0.8119 (1)	ANFIS	2.1282 *	0.571 (1)	ANFIS	2.1505 *	0.369 (1)	NARNN	2.2729 *	0.4898 (1)

Table A5. *Cont.*

Type	Period	1st Season									
	Site	Site 1		Site	Site 2		Site	Site 3		Site	Site 4	
	Model	DM Test	WRS Test	Model	DM Test	WRS Test	Model	DM Test	WRS Test	Model	DM Test	WRS Test
Wind Power	LSTM	2.1095 *	0.617 (1)	LSTM	2.1545 *	0.2666 (1)	Elman	1.8865 **	0.1524 (1)	Elman	2.0134 *	0.3397 (1)
	Elman	2.0571 *	0.7218 (1)	Elman	2.0155 *	0.2679 (1)	LSTM	1.8103 **	0.2156 (1)	BPNN	2.1494 *	0.4345 (1)
	BPNN	2.1123 *	0.8302 (1)	BPNN	2.0564 *	0.442 (1)	BPNN	1.8667 **	0.6435 (1)	RBFNN	2.0748 *	0.8048 (1)
	RBFNN	2.0746 *	0.9939 (1)	SVM	1.9941 **	0.7566 (1)	SVM	1.8281 **	0.9013 (1)	ANFIS	2.0411 *	0.8842 (1)
	SVM	2.0468 *	0.9744 (1)	RBFNN	1.9628 *	0.992 (1)	RBFNN	1.8860 **	0.9017 (1)	GRNN	2.0735 *	0.6124 (1)

Note: * is at the 10% significance level. ** is at the 5% significance level. *** is at the 1% significance level. (0) there is difference between two sample at the 5% significance level. (1) there is no difference between two sample at the 5% significance level.

References

1. GWEC | GLOBAL WIND REPORT 2021. 2021. Available online: https://gwec.net/wp-content/uploads/2021/03/GWEC-Global-Wind-Report-2021.pdf (accessed on 5 May 2021).
2. Liu, H.; Tian, H.-Q.; Li, Y.-F. Four wind speed multi-step forecasting models using extreme learning machines and signal de-composing algorithms. *Energy Convers. Manag.* **2015**, *100*, 16–22. [CrossRef]
3. Selig, M.S.; Tangler, J.L. Development of a multipoint inverse design method for horizontal axis wind turbines. *Wind. Eng.* **1995**, *19*, 91–105.
4. Lee, S. Inverse design of horizontal axis wind turbine blades using a vortex line method. *Wind Energy* **2015**, *18*, 253–266. [CrossRef]
5. Moghadassian, B.; Sharma, A. Inverse Design of Single-A and Multi-Rotor Horizontal Axis Wind Turbine Blades Using Com-Putational Fluid Dynamics. *J. Sol. Energy Eng.* **2017**, *140*, 021003. [CrossRef]
6. Tahani, M.; Kavari, G.; Masdari, M.; Mirhosseini, M. Aerodynamic design of horizontal axis wind turbine with innovative local linearization of chord and twist distributions. *Energy* **2017**, *131*, 78–91. [CrossRef]
7. Liu, X.; Wang, L.; Tang, X. Optimized linearization of chord and twist angle profiles for fixed-pitch fixed-speed wind turbine blades. *Renew. Energy* **2013**, *57*, 111–119. [CrossRef]
8. Soman, S.S.; Zareipour, H.; Malik, O.; Mandal, P. A review of wind power and wind speed forecasting methods with different timehorizons. In Proceedings of the North-American Power Symposium 2010, Arlington, TX, USA, 26–28 September 2010; pp. 1–7. [CrossRef]
9. Zhang, S.; Chen, Y.; Xiao, J.; Zhang, W.; Feng, R. Hybrid wind speed forecasting model based on multivariate data secondary decomposition approach and deep learning algorithm with attention mechanism. *Renew. Energy* **2021**, *174*, 688–704. [CrossRef]
10. Jacondino, W.D.; Nascimento, A.L.D.S.; Calvetti, L.; Fisch, G.; Beneti, C.A.A.; da Paz, S.R. Hourly day-ahead wind power forecasting at two wind farms in northeast Brazil using WRF model. *Energy* **2021**, *230*, 120841. [CrossRef]
11. Pearre, N.S.; Swan, L.G. Statistical approach for improved wind speed forecasting for wind power production. *Sustain. Energy Technol. Assess.* **2018**, *27*, 180–191. [CrossRef]
12. Jahangir, H.; Golkar, M.A.; Alhameli, F.; Mazouz, A.; Ahmadian, A.; Elkamel, A. Short-term wind speed forecasting framework based on stacked denoising auto-encoders with rough ANN. *Sustain. Energy Technol. Assess.* **2020**, *38*, 100601. [CrossRef]
13. Dong, Y.; Zhang, L.; Liu, Z.; Wang, J. Integrated Forecasting Method for Wind Energy Management: A Case Study in China. *Processes* **2019**, *8*, 35. [CrossRef]
14. Jiang, P.; Liu, Z.; Niu, X.; Zhang, L. A combined forecasting system based on statistical method, artificial neural networks, and deep learning methods for short-term wind speed forecasting. *Energy* **2021**, *217*, 119361. [CrossRef]
15. Brabec, M.; Craciun, A.; Dumitrescu, A. Hybrid numerical models for wind speed forecasting. *J. Atmos. Sol. Terr. Phys.* **2021**, *220*, 105669. [CrossRef]
16. Zhao, J.; Guo, Z.; Guo, Y.; Lin, W.; Zhu, W. A self-organizing forecast of day-ahead wind speed: Selective ensemble strategy based on numerical weather predictions. *Energy* **2021**, *218*, 119509. [CrossRef]
17. Al-Yahyai, S.; Charabi, Y.; Gastli, A. Review of the use of Numerical Weather Prediction (NWP) Models for wind energy as-sessment. *Renew. Sustain. Energy Rev.* **2010**, *14*, 3192–3198. [CrossRef]
18. Mu, M.U.; Chen, B. Methods and Uncertainties of Meteorological Forecast. *Meteorol. Mon.* **2011**, *37*, 1–13. [CrossRef]
19. Khodayar, M.; Wang, J. Spatio-Temporal Graph Deep Neural Network for Short-Term Wind Speed Forecasting. *IEEE Trans. Sustain. Energy* **2018**, *10*, 670–681. [CrossRef]
20. Lu, P.; Ye, L.; Zhong, W.; Qu, Y.; Zhai, B.; Tang, Y.; Zhao, Y. A novel spatio-temporal wind power forecasting framework based on multi-output support vector machine and optimization strategy. *J. Clean. Prod.* **2020**, *254*, 119993. [CrossRef]
21. Sun, M.; Feng, C.; Zhang, J. Conditional aggregated probabilistic wind power forecasting based on spatio-temporal correlation. *Appl. Energy* **2019**, *256*, 113842. [CrossRef]
22. Liu, Y.; Qin, H.; Zhang, Z.; Pei, S.; Jiang, Z.; Feng, Z.; Zhou, J. Probabilistic spatiotemporal wind speed forecasting based on a variational Bayesian deep learning model. *Appl. Energy* **2020**, *260*, 114259. [CrossRef]
23. Ma, X.; Jin, Y.; Dong, Q. A generalized dynamic fuzzy neural network based on singular spectrum analysis optimized by brain storm optimization for short-term wind speed forecasting. *Appl. Soft Comput.* **2017**, *54*, 296–312. [CrossRef]
24. Niu, T.; Wang, J.; Zhang, K.; Du, P. Multi-step-ahead wind speed forecasting based on optimal feature selection and a modified bat algorithm with the cognition strategy. *Renew. Energy* **2018**, *118*, 213–229. [CrossRef]
25. Iversen, E.B.; Morales, J.; Møller, J.K.; Madsen, H. Short-term probabilistic forecasting of wind speed using stochastic differential equations. *Int. J. Forecast.* **2016**, *32*, 981–990. [CrossRef]
26. Torres, J.; García, A.; de Blas, M.; Francisco, A. Forecast of hourly average wind speed with ARMA models in Navarre (Spain). *Sol. Energy* **2005**, *79*, 65–77. [CrossRef]
27. Erdem, E.; Shi, J. ARMA based approaches for forecasting the tuple of wind speed and direction. *Appl. Energy* **2011**, *88*, 1405–1414. [CrossRef]
28. Shukur, O.B.; Lee, M. Daily wind speed forecasting through hybrid KF-ANN model based on ARIMA. *Renew. Energy* **2015**, *76*, 637–647. [CrossRef]

29. Yang, D.; Sharma, V.; Ye, Z.; Lim, L.I.; Zhao, L.; Aryaputera, A.W. Forecasting of global horizontal irradiance by exponential smoothing, using decompositions. *Energy* **2015**, *81*, 111–119. [CrossRef]
30. Zuluaga, C.; Álvarez, M.A.; Giraldo, E. Short-term wind speed prediction based on robust Kalman filtering: An experimental comparison. *Appl. Energy* **2015**, *156*, 321–330. [CrossRef]
31. Cavalcante, L.; Bessa, R.J.; Reis, M.; Browell, J. LASSO vector autoregression structures for very short-term wind power forecasting. *Wind Energy* **2017**, *20*, 657–675. [CrossRef]
32. Ziel, F.; Croonenbroeck, C.; Ambach, D. Forecasting wind power—Modeling periodic and non-linear effects under conditional heteroscedasticity. *Appl. Energy* **2016**, *177*, 285–297. [CrossRef]
33. Bessa, R.; Trindade, A.; Miranda, V. Spatial-Temporal Solar Power Forecasting for Smart Grids. *IEEE Trans. Ind. Informatics* **2015**, *11*, 232–241. [CrossRef]
34. Wang, J.; Heng, J.; Xiao, L.; Wang, C. Research and application of a combined model based on multi-objective optimization for multi-step ahead wind speed forecasting. *Energy* **2017**, *125*, 591–613. [CrossRef]
35. Li, X.; Yang, D.; Yang, J.; Zheng, G.; Han, G.; Nan, Y.; Li, W. Analysis of coastal wind speed retrieval from CYGNSS mission using artificial neural network. *Remote Sens. Environ.* **2021**, *260*, 112454. [CrossRef]
36. Prasad, S.; Nguyen-Huy, T.; Deo, R. Support vector machine model for multistep wind speed forecasting. *Predict. Model. Energy Manag. Power Syst. Eng.* **2020**, 335–389. [CrossRef]
37. Kalajdjieski, J.; Zdravevski, E.; Corizzo, R.; Lameski, P.; Kalajdziski, S.; Pires, I.; Garcia, N.; Trajkovik, V. Remote Sensing Air Pollution Prediction with Multi-Modal Data and Deep Neural Networks. *Remote Sens.* **2020**, *12*, 4142. [CrossRef]
38. Jiang, P.; Yang, H.; Heng, J. A hybrid forecasting system based on fuzzy time series and multi-objective optimization for wind speed forecasting. *Appl. Energy* **2019**, *235*, 786–801. [CrossRef]
39. Zhao, J.; Guo, Z.-H.; Su, Z.-Y.; Zhao, Z.-Y.; Xiao, X.; Liu, F. An improved multi-step forecasting model based on WRF ensembles and creative fuzzy systems for wind speed. *Appl. Energy* **2016**, *162*, 808–826. [CrossRef]
40. Naik, J.; Dash, S.; Dash, P.; Bisoi, R. Short term wind power forecasting using hybrid variational mode decomposition and multi-kernel regularized pseudo inverse neural network. *Renew. Energy* **2018**, *118*, 180–212. [CrossRef]
41. Liu, Z.; Hara, R.; Kita, H. Hybrid forecasting system based on data area division and deep learning neural network for short-term wind speed forecasting. *Energy Convers. Manag.* **2021**, *238*, 114136. [CrossRef]
42. Aly, H.H. A proposed intelligent short-term load forecasting hybrid models of ANN, WNN and KF based on clustering techniques for smart grid. *Electr. Power Syst. Res.* **2020**, *182*, 106191. [CrossRef]
43. Wang, D.; Luo, H.; Grunder, O.; Lin, Y. Multi-step ahead wind speed forecasting using an improved wavelet neural network combining variational mode decomposition and phase space reconstruction. *Renew. Energy* **2017**, *113*, 1345–1358. [CrossRef]
44. Huang, X.; Wang, J.; Huang, B. Two novel hybrid linear and nonlinear models for wind speed forecasting. *Energy Convers. Manag.* **2021**, *238*, 114162. [CrossRef]
45. Du, P.; Wang, J.; Guo, Z.; Yang, W. Research and application of a novel hybrid forecasting system based on multi-objective optimization for wind speed forecasting. *Energy Convers. Manag.* **2017**, *150*, 90–107. [CrossRef]
46. Jiang, P.; Wang, Y.; Wang, J. Short-term wind speed forecasting using a hybrid model. *Energy* **2017**, *119*, 561–577. [CrossRef]
47. Hu, J.; Wang, J.; Xiao, L. A hybrid approach based on the Gaussian process with t-observation model for short-term wind speed forecasts. *Renew. Energy* **2017**, *114*, 670–685. [CrossRef]
48. Corizzo, R.; Ceci, M.; Fanaee-T, H.; Gama, J. Multi-aspect renewable energy forecasting. *Inf. Sci.* **2021**, *546*, 701–722. [CrossRef]
49. Cai, C.; Tao, Y.; Zhu, T.; Deng, Z. Short-Term Load Forecasting Based on Deep Learning Bidirectional LSTM Neural Network. *Appl. Sci.* **2021**, *11*, 8129. [CrossRef]
50. Han, Q.; Meng, F.; Hu, T.; Chu, F. Non-parametric hybrid models for wind speed forecasting. *Energy Convers. Manag.* **2017**, *148*, 554–568. [CrossRef]
51. Zhou, Q.; Wang, C.; Zhang, G. A combined forecasting system based on modified multi-objective optimization and sub-model selection strategy for short-term wind speed. *Appl. Soft Comput.* **2020**, *94*, 106463. [CrossRef]
52. Wang, C.; Zhang, H.; Ma, P. Wind power forecasting based on singular spectrum analysis and a new hybrid Laguerre neural network. *Appl. Energy* **2020**, *259*, 114139. [CrossRef]
53. Wang, S.; Zhang, N.; Wu, L.; Wang, Y. Wind speed forecasting based on the hybrid ensemble empirical mode decomposition and GA-BP neural network method. *Renew. Energy* **2016**, *94*, 629–636. [CrossRef]
54. Song, J.; Wang, J.; Lu, H.Y. A novel combined model based on advanced optimization algorithm for short-term wind speed forecasting. *Appl. Energy* **2018**, *215*, 643–658. [CrossRef]
55. Wang, C.; Zhang, S.; Xiao, L.; Fu, T. Wind speed forecasting based on multi-objective grey wolf optimisation algorithm, weighted information criterion, and wind energy conversion system: A case study in Eastern China. *Energy Convers. Manag.* **2021**, *243*, 114402. [CrossRef]
56. Haynes, W. Wilcoxon Rank Sum Test. In *Encyclopedia of Systems Biology*; Dubitzky, W., Wolkenhauer, O., Cho, K.-H., Yokota, H., Eds.; Springer: New York, NY, USA, 2013; pp. 2354–2355.
57. Jiang, P.; Li, R.; Li, H. Multi-objective algorithm for the design of prediction intervals for wind power forecasting model. *Appl. Math. Model.* **2019**, *67*, 101–122. [CrossRef]
58. Yang, W.; Wang, J.; Lu, H.; Niu, T.; Du, P. Hybrid wind energy forecasting and analysis system based on divide and conquer scheme: A case study in China. *J. Clean. Prod.* **2019**, *222*, 942–959. [CrossRef]

59. Jiang, P.; Li, C.; Li, R.; Yang, H. An innovative hybrid air pollution early-warning system based on pollutants forecasting and Extenics evaluation. *Knowledge-Based Syst.* **2019**, *164*, 174–192. [CrossRef]
60. Wang, J.; Niu, T.; Lu, H.; Yang, W.; Du, P. A Novel Framework of Reservoir Computing for Deterministic and Probabilistic Wind Power Forecasting. *IEEE Trans. Sustain. Energy* **2019**, *11*, 337–349. [CrossRef]
61. Tian, C.; Hao, Y. Point and interval forecasting for carbon price based on an improved analysis-forecast system. *Appl. Math. Model.* **2020**, *79*, 126–144. [CrossRef]
62. Liu, Z.; Jiang, P.; Zhang, L.; Niu, X. A combined forecasting model for time series: Application to short-term wind speed fore-casting. *Appl. Energy* **2019**, *259*, 114137. [CrossRef]